



Institute of Biomechanics  
Center of Biomedical Engineering  
Kronesgasse 5-I  
8010 Graz, Austria

## **Master Thesis**

# Characterization of the Orthotropic Mechanical Behavior of Human Myocardium by Triaxial Shear Testing

to achieve the degree of  
Master of Science

**Author:** Carina Luttenberger, BSc

**Supervisor:** Gerhard Sommer, PhD

**Head of Institute:** Professor Gerhard A. Holzapfel, PhD

May 19, 2015

# Contents

<b>1</b>	<b>Introduction</b>	<b>1</b>
1.1	Motivation . . . . .	1
1.1.1	What Is Biomechanics? . . . . .	1
1.1.2	Aim . . . . .	2
1.2	The Heart - Anatomy and Biomechanics . . . . .	3
1.2.1	Anatomy . . . . .	3
1.2.1.1	General . . . . .	3
1.2.1.2	Myocardium . . . . .	4
1.2.2	Biomechanics . . . . .	7
1.2.2.1	Biomechanics of Soft Biological Tissue . . . . .	7
1.2.2.2	Simple Shear . . . . .	8
<b>2</b>	<b>Materials &amp; Methods</b>	<b>12</b>
2.1	Materials . . . . .	12
2.1.1	Collection and Storage of Materials . . . . .	13
2.1.2	Solution for Storage and Testing . . . . .	13
2.1.2.1	Cardioplegic Solution (CPS) . . . . .	13
2.1.2.2	BDM - 2,3-Butanedione Monoxime . . . . .	14
2.1.2.3	Formaldehyde . . . . .	15
2.2	Methods . . . . .	16
2.2.1	Myocardial Samples . . . . .	16
2.2.1.1	Tools for Heart and Specimen Preparation . . . . .	16
2.2.1.2	Heart Dissection . . . . .	17
2.2.1.3	Preparation of the Cubic Heart Specimens . . . . .	19
2.2.1.4	The FSN-Coordinate System . . . . .	20
2.2.1.5	Preparation of three Cubic Specimens . . . . .	21
2.2.2	Shear Test Device . . . . .	23
2.2.2.1	Instruments . . . . .	23
2.2.2.2	Setup of the Triaxial Shear Test Device . . . . .	24
2.2.3	Shear Testing . . . . .	26
2.2.3.1	Fixation of Specimen into the Triaxial Shear Device . . . . .	26
2.2.3.2	Testing Protocol . . . . .	27
2.2.4	Data Analysis . . . . .	30
2.2.4.1	MATLAB®Data Evaluation Script . . . . .	30

---

<b>3</b>	<b>Results</b>	<b>32</b>
3.1	Results of the Shear Test . . . . .	33
3.2	Example of Failed Testing . . . . .	39
3.3	Statistical Analysis . . . . .	41
<b>4</b>	<b>Discussion</b>	<b>46</b>
4.1	General Discussion . . . . .	46
4.2	Limitations . . . . .	48
4.3	Pathological Aspects . . . . .	48
4.4	Conclusion . . . . .	49
	<b>Bibliography</b>	<b>51</b>

# List of Figures

1.1	The 10 leading causes of death in the world . . . . .	1
1.2	The structure of the human heart . . . . .	4
1.3	The geometry of fibers and the laminar structure of the heart . . . . .	5
1.4	Schematic illustration of fiber orientation within the heart and the tissue sample . . . . .	6
1.5	Simple shear of a specimen . . . . .	8
1.6	FSN coordinate system of a specimen . . . . .	9
1.7	Simple shear of a block . . . . .	10
2.1	Ion concentrations in and around of a cardiac myocyte . . . . .	14
2.2	Tools for heart and specimen preparation . . . . .	16
2.3	Example of a whole heart with and without the atrium . . . . .	17
2.4	Exemplary presentation of the dissection of the heart . . . . .	18
2.5	Septum, left ventricle and right ventricle individually . . . . .	18
2.6	Simplified representation of the heart . . . . .	19
2.7	Representation of a cubic specimen within the heart . . . . .	20
2.8	Six modes of simple shear according to the FSN coordinates . . . . .	21
2.9	Cubic specimen in FSFN-mode . . . . .	22
2.10	Cubic specimen ready for testing . . . . .	22
2.11	Block diagram of the experimental setup . . . . .	23
2.12	Triaxial shear testing device (middle) with the computer (rleft) and three controlling towers (Z, Y, X) (right). . . . .	24
2.13	(A) shows the shear test device (TRIAX) and (B) the tissue bath filled with cardaplegic solution and a cubic specimen fixed between the upper and lower stamp . . . . .	25
2.14	TestXPertII Layout-Assistant for setting the sample properties before testing	28
2.15	TestXPertII Layout-Assistant for setting the exact specimen dimensions before testing . . . . .	28
2.16	Preconditioning and data recording cycles af a typical sample . . . . .	29
2.17	Three cubic specimens for six possible modes of simple shear with the correct marking (violet dots on the top) in two corners . . . . .	29
2.18	Overview of the MATLAB®GUI . . . . .	30
2.19	Plot of typical shear stress vs. amount of shear curves (FS- and FN-modes) within the MATLAB® editing interface . . . . .	31



---

3.1	Relationship of shear stress and amount of shear during testing cycles of sinusoidal simple shear in NF/NS mode. Maximum amount of shear is increased from 0.1 to 0.5. . . . .	32
3.2	Shear stress vs. amount of shear curve of a left ventricle (HH#29) in FN/FS (top), SF/SN (middle) and NF/NS mode (bottom) increasing from 10% to 50%. . . . .	36
3.3	Shear stress vs. amount of shear curve of a right ventricle (HH#29) in FN/FS (top), SF/SN (middle) and NF/NS mode (bottom) increasing from 10% to 50%. . . . .	37
3.4	Shear stress vs. amount of shear curve of a septum (HH#28) in FN/FS (top), SF/SN (middle) and NF/NS mode (bottom) increasing from 10% to 50%. . . . .	38
3.5	Example of a failed test (NF/NS mode of HH#32 <sub>LV</sub> ) . . . . .	39
3.6	Left ventricle (HH#32) with SN/SF mode. . . . .	40
3.7	All samples for all six modes at an amount of shear of 0.1. . . . .	42
3.8	All samples for all six modes at an amount of shear of 0.2. . . . .	42
3.9	All samples for all six modes at an amount of shear of 0.3. . . . .	43
3.10	All samples for all six modes at an amount of shear of 0.4. . . . .	43
3.11	All samples for all six modes at an amount of shear of 0.5. . . . .	43
3.12	Average in FS/FN mode at 10–50% amount of shear . . . . .	44
3.13	Average in SF/SN mode at 10–50% amount of shear . . . . .	44
3.14	Average in NS/NF mode at 10–50% amount of shear . . . . .	45
4.1	Midlines of shear stress-displacement loops over all 6 hearts tested in Dokos et al. (2002) . . . . .	47

# List of Tables

2.1	Patient related heart data . . . . .	12
3.1	Overview of relevant information of the tested heart specimens with regard to the shear test . . . . .	33
3.1	Overview: Continuation . . . . .	34
3.2	Statistical overview of all eleven samples. . . . .	41
3.3	Overview of reasons of exclusion of heart #30, #32, #36 and #37. . . . .	41
4.1	Patient related heart data . . . . .	49

# Abstract

Cardiovascular diseases are the leading cause of death in Austria which affects about 34.000 people per year. The mechanical properties and the underlying mechanics are essential for the understanding of the structure and the functions of the human heart tissue. Further, the knowledge of the effects which act on the heart helps us to figure out the mechanism of disease development. Consequently, the field of heart research is an important area of biomechanics.

The present master thesis is part of a major project of the Institute of Biomechanics, Graz University of Technology. The aim is to characterize the mechanical properties of the human myocardium in order to develop a finite element simulation model of the behaviour of healthy and diseased myocardia. Therefore, biaxial tensile and triaxial shear tests are performed and the microstructure is investigated.

Initially this work was motivated by the previous study on porcine tissue of Dokos et al. (2002). This study had the aim to develop a standardized protocol for the triaxial investigation of shear properties.

This thesis dealt with the correct dissection and preparation of three cubic heart samples ( $3 \times 3 \times 3$  mm) and the alignment of the axis within the FSN-coordinate system. The purpose was to characterize the already assumed mechanical properties and the behaviour under shear of the human myocardium. For this, the samples were investigated with the help of the triaxial shear testing device located in the Institute of Biomechanics. Further, the fiber and sheet orientations were examined in order to find out if the orientation has a contribution to the mechanical behaviour of the human heart.

In the course of this thesis human hearts (mostly only pieces of the organ due to the high demand for human tissue) were received from the Department of Transplant Surgery, Medical University of Graz. In total 11 different human hearts and as a result 20 heart samples and over 60 cubic specimens were tested. The human myocardium showed the characteristic properties of soft biological tissue. Nonlinear and viscoelastic behaviour with a strong anisotropy. Meaning higher resistance to shear performed in a specific direction or more precisely in myofiber direction. The stiffness of the tissue decreases as follows:  $F > S > N$  (with F being the mean myofiber orientation, S the direction transverse to the fiber axis within the layers and N the sheet normal direction). The results are therefore conform with those of Dokos et al. (2002) and the literature.

# Zusammenfassung

Kardiovaskuläre Erkrankungen sind die häufigste Todesursache in Österreich und betreffen um die 34.000 Menschen pro Jahr. Die mechanischen Eigenschaften und die zugrundeliegende Mechanik sind essentiell für das Verständnis der Struktur und Funktion von humanen Herzen. Weiters hilft uns das Wissen über die Effekte die auf das Herz wirken, die Mechanismen der Krankheitsentstehung besser zu verstehen. Somit ist die Herzforschung ein wichtiger Bereich der Biomechanik.

Diese Masterarbeit ist ein Teil eines größeren Projektes am Institut für Biomechanik der Technischen Universität Graz. Das Ziel ist es, die mechanischen Eigenschaften des humanen Myokards zu charakterisieren um in Folge eine Finite Elemente Methoden-Simulation von gesunden und erkrankten Herzwänden zu erstellen. Dafür wurden biaxiale Dehn- und triaxiale Scherversuche durchgeführt und die Mikrostruktur untersucht.

Den Anstoß für diese Arbeit gab ursprünglich die Studie von Dokos et al. (2002). Er untersuchte die mechanischen Eigenschaften der Myokarde von Schweinen. Das Ziel war es, ein standardisiertes Protokoll für die Untersuchung von Schereigenschaften zu entwickeln.

Diese Arbeit behandelt die korrekte Präparation von würfelförmigen Proben ( $3 \times 3 \times 3$  mm) und die Ausrichtung der Achsen mit dem FSN-Koordinatensystem. Das hat das Ziel die schon angenommenen mechanischen Eigenschaften und das Verhalten unter Scherung von Herzwänden zu charakterisieren. Dazu wurde eine triaxiale Scherapparatur am Institut für Biomechanik verwendet. Weiters wurde die Faser- und Schichtausrichtung bestimmt, um herauszufinden ob diese Orientierung Auswirkungen auf das mechanische Verhalten hat.

Im Zuge dieser Arbeit wurden Herzen (meistens nur Teile des Organs aufgrund der hohen Nachfrage nach humanen Gewebe) von der klinischen Abteilung für Transplantationschirurgie der Medizinischen Universität Graz erhalten. Insgesamt wurden elf verschiedene Herzen und infolgedessen 20 Gewebeproben und über 60 Würfel getestet. Das Myokard zeigte die charakteristischen Eigenschaften von weichem biologischen Gewebe. Nicht-lineares und viskoses Verhalten mit einer starken Richtungsabhängigkeit (Anisotropie). Das bedeutet einen höheren Widerstand gegenüber Scherung in eine spezielle Richtung, nämlich in die der Fasern. Die Steifigkeit des Gewebes in Abhängigkeit der Orientierung der Mikrostrukturen nimmt wie folgt ab:  $F > S > N$  (wobei F die Richtung der Fasern darstellt, S die Richtung der Schichten und N liegt normal zu Orientierung der Schichten).

# Acknowledgment

I want to offer my sincere thanks to everyone who supported me during this thesis and throughout the years of university.

First of all, I would like to give special thanks to my mentor Dipl.-Ing. Dr.techn. Gerhard SOMMER for his great support and supervision during my whole master thesis. Thank you Gerhard for your help and patience the last year.

I also would like to thank the Head of the Institute of Biomechanics Univ.-Prof. Dipl.-Ing. Dr.techn. Gerhard A. HOLZAPFEL, for the opportunity of writing this master thesis at his Institute and for providing the laboratory facilities.

Further, I want to thank all who accompanied me over the time at university. Without you it would not have been such a great time.

A very special thanks is due to my partents, Anna und Erich, who ALWAYS support me in all situations. Thank you so much!

And last but not least, I want to thank my boyfriend Dennis who helped me with his advice and actions. Thank you for being so patient!

# 1 Introduction

## 1.1 Motivation

### 1.1.1 What Is Biomechanics?

‘Biomechanics is mechanics applied to biology.’ [1]

In general biomechanics analyses any dynamic system. Consequently, it wants to understand the mechanics of any living system and can also be defined as the application of mechanics to answer questions in medicine and biology [1]. We owe biomechanics that we understand many of the biophysical phenomena that act at molecular, cellular, tissue, organ and organism levels [2].

Biomechanics plays a major role solving clinical problems in any field of research. These days biomechanics take part in the modern progress of medical science and technology and therefore biomechanics is closely related to diagnosis, prosthesis and surgery. As a consequence it helps us to understand, prevent and predict diseases, such as cardiovascular diseases (CVD) - the leading cause of death in Austria and all over the world, as shown in Fig. 1.1 [1].

More people die from cardiovascular diseases than for any other reason. According to Statistik Austria in 2012, 33.931 people (42,7%) died due to cardiovascular diseases and 20.266 (25,5%) due to cancer, in Austria. Thus, these two diseases cause seven out of ten deaths [3].

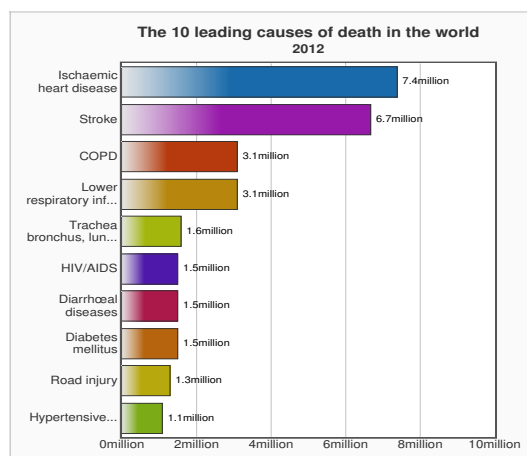


Figure 1.1: The 10 leading causes of death in the world 2012. Adapted from [4].

In particular, it is very important to figure out the stress-strain relationship in the heart in *ex vivo* for understanding the mechanical properties of the intact human heart. The mechanical characterization of it leads to a better understanding of the deformation of the beating heart, because these stress and strain fields are directly related to the cardiac wall motion and reproduce the local contractile state. Further, it can be understood how diseased or ischemic regions can impair the pumping ability [5, 6]. So if we knew the stresses and strains in and around an infarction, the cardiologist could identify the region and its changed properties, the dimension of damage, the perspective of recovery and the vulnerability to a failure like an aneurysm [7]. Thus, a mathematical model which could forecast the relation between pathology and deformation would be a very useful clinical tool in diagnosis. It could be used in diagnosis and to select the right tool for intervention by simulating interventions beforehand [8].

In summary, biomechanics and constitutive modeling are useful tools for understanding the effects which act on the human heart and help us to figure out the mechanism of disease development.

### **1.1.2 Aim**

This work is just a small part of a bigger project which is to characterize the mechanical properties of the human myocardium by biaxial tensile and triaxial shear testing. Furthermore, the microstructure of the myocardium is investigated. This is done in order to derive new constitutive descriptors and linked parameters for developing more accurate numerical (finite element method - FEM) simulations [6].

In very simple terms the whole project consists of:

1. Determination of mechanical properties of the human myocardium
2. Determination of microstructure of the human myocardium
3. Verification and modification of existing constitutive models

The aim of this work is to characterize the mechanical properties and shear behavior, respectively, of passive human ventricular myocardium.

## 1.2 The Heart - Anatomy and Biomechanics

‘The heart is the beginning of life; the sun of the microcosm, even as the sun in his turn might well be designated the heart of the world.’ (William Harvey)

### 1.2.1 Anatomy

#### 1.2.1.1 General

Principally the heart is not more than a hollow muscle. The heart muscle has a weight of about 250–400 g, is approximately as big as the own fist and has the same shape [9].

The function of the heart is simple and basically mechanical - to pump blood through the whole body [2]. Thereby, oxygen and nutrients are delivered and waste (e.g. carbon dioxide, ...) is removed from each organ.

From a functional standpoint, the heart is split in two "heart halves" - which pump in different parts of the blood circulation.

#### 1. The ‘right heart’:

In simple terms, it pumps blood from the body to the lung. The right heart, as well as the left heart, consists of two chambers. The right atrium, which collects the oxygen-poor blood that returns from the body via the inferior and superior vena cave. And the right ventricle which pumps the blood through the pulmonary valve and the pulmonary arteries to the lung.

#### 2. The ‘left heart’:

It pumps in the opposite direction - from the lung to the organs of the body in a similar procedure. The left atrium collects the oxygen-rich blood from the lung via the pulmonary veins and the left ventricle pumps blood through the aortic valve and the aorta to the remainder of the body. As we can see, the ventricles are the predominant pumping chambers while the atrium is mainly a temporary blood reservoir for the ventricles.

Right and left heart are combined but strictly separated from each other. Thus there is no connection within the heart. For the separation of the two halves, interventricular septum is responsible [2, 7, 9]. In Fig. 2.2 you can see the structure of a human heart.

The left ventricle is thick-walled due to the fact that it pumps blood at physiologically high pressures (up to 15kPa or 110mmHg) to ensure the blood flow to distal locations throughout the body. In contrast, the right ventricle has thinner walls, because it pumps blood with low pressures (one seventh the pressure of the LV) just to the lungs [10].

The heart wall has a three-layered architecture: the endocardium is a smooth inner layer and is important for the low friction of the blood within the heart; the epicardium is the outer layer and responsible for a good relocatability of the heart and the surrounding area; and the myocardium [9].



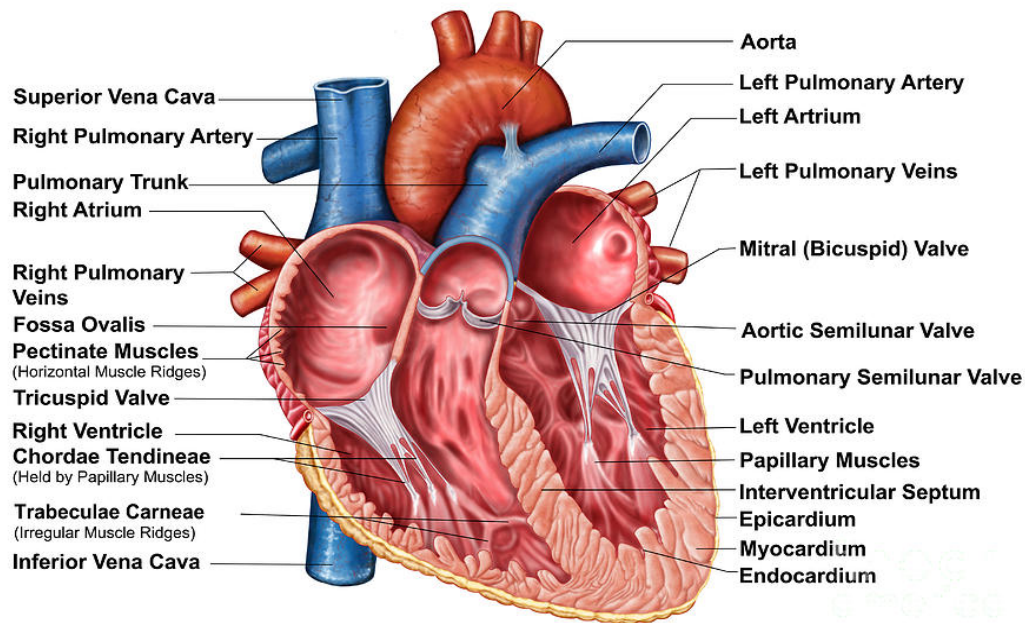


Figure 1.2: The structure of the human heart. Adapted from [11].

### 1.2.1.2 Myocardium

The myocardium is the most important layer, due to the fact that it endows the heart with its ability to pump blood. It is the thickest layer and consists of cells that are mechanically and electrically connected to each other [2, 9].

The structure of the ventricular wall is highly organized and complex. It is composed of several types of cells that include cardiac cells, smooth muscle cells and fibroblasts. But the most important and fundamental contractile cell is the myocyte. The myocytes are arranged into parallel muscle fibers, which are then embedded in the extracellular matrix to preserve the tissue architecture during large deformation like contractile motion. The extracellular matrix prevents muscle fiber rupture or slippage and consists of collagen, mainly of type I and III where type I corresponds to highly tensile strength material and type III to highly deformable material [2, 12–14]. The myocardium is composed of separated layers of myocardial muscle fibers which are tightly bound by type III collagen called endomy-sium. These sheets are then physically separated and loosely connected by a coiled bundle of type I collagen fibers called perimysium, giving them the ability to slide over each other. Thus cover the surface of muscle layers and thereby define the laminar architecture. The potential space between the sheets is called cleavage planes. Sheets are four to six cells thick and their orientation is commonly normal to the ventricular surface and run almost parallel with one another [5, 10, 15]. Figure 1.3 shows this laminar structure of the myocardium.

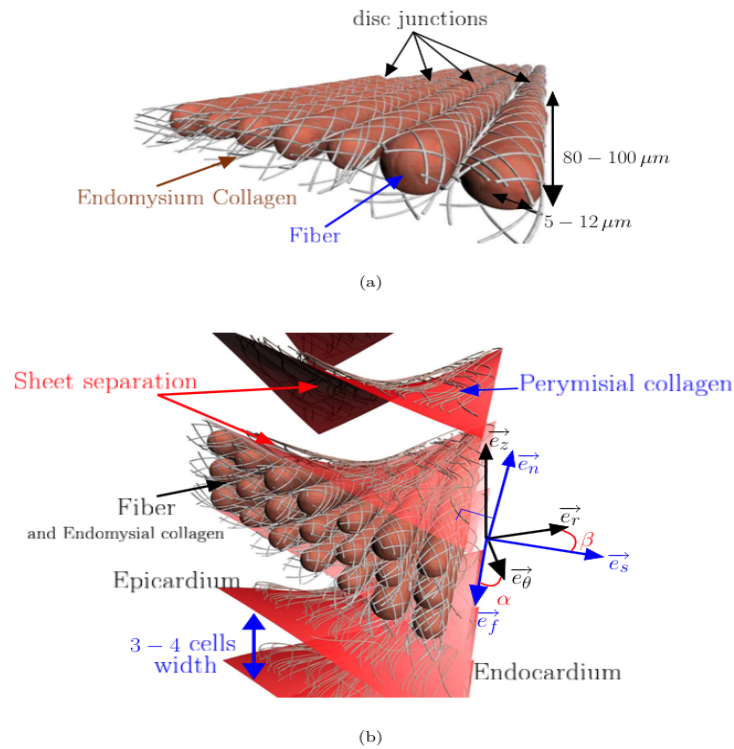


Figure 1.3: Panel (a) shows the geometry of the fiber and endomysial collagen in the heart. Panel (b) shows the lamellar structure. Illustrations adapted from [14].

Within the left ventricle the fibers form a helical structure and thereby the orientation of the muscle fibers change with position in the wall from epicardium to endocardium, as you can see in Fig. 1.4 (a). Muscle fiber orientation is quantified by the helix fiber angle  $\alpha$  and varies between  $+60^\circ$  and  $-60^\circ$  across the wall [2, 14, 16]. The muscle fibers follow a transition from negative angles in the epicardium, to a circumferential direction in the midwall and then reaching an axial orientation in the endocardium [5].

The organization of cardiac myocytes and myolaminae is the key element of myocardial structure and play an important role in the mechanical as well as the functional performance of the heart. Large shear deformation during the filling phase and ejection are aligned along myocardial laminae and the myocardium prefers shear in directions parallel with this structure [15].

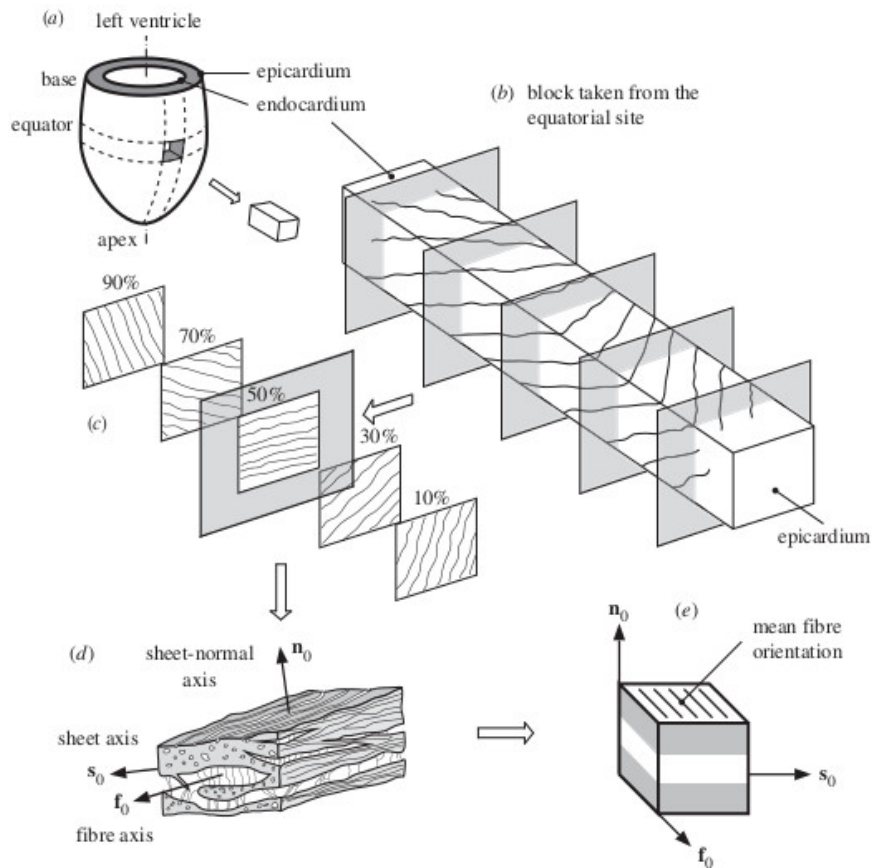


Figure 1.4: Representation of the fiber orientation within the left ventricle:(a) the left ventricle and a cutout (specimen); (b) the microstructure through the specimen from the epicardium to the endocardium; (c) the changing of the fibre orientation; (d) the layers of myocytes and the collagen fibres between the sheets; (e) a cube of layered tissue. Adapted from [17].

## 1.2.2 Biomechanics

Now we want to discuss the biomechanical properties of the human heart or, to be more accurate, the myocardium. Therefore, we pay more attention to soft biological tissues. We can split biological tissue into hard tissue like bone and tooth and soft tissue like skin, blood vessels and muscles, such as the human myocardium. For this reason the heart owns the same biomechanical behaviour and characteristics [18].

### 1.2.2.1 Biomechanics of Soft Biological Tissue

The mechanical properties of soft biological tissues are required and essential for biomechanics. Each tissue has its own set of unique characteristics but general behaviours are common to many of them. These are the properties we want to discuss.

#### 1. Inhomogeneous Structure

Cells and intracellular substances are the main components of soft biological tissues, whereby the intracellular substance consists of connective tissues such as collagen and elastin, and ground substance. These components have different properties from chemical and physical nature and their composition differs from tissue to tissue and even from site to site. Therefore, the mechanical properties are inhomogeneous and depend on tissue and on site.

#### 2. Nonlinear Large Deformation

Each component of soft biological tissue shows nonlinear behaviour, this means that the stress-strain behaviour is nonlinear. The nonlinearity increases with the assembly of them into a tissue. Thus, biological soft tissues are nonlinear, geometrically and mechanically.

#### 3. Anisotropy

As we know, collagen and elastin are, among other things, important components of soft biological tissue. They are long-chained high polymers and are by itself anisotropic. That means that they depend on the orientation to operate most effectively. At low stretches the myocardial response is independent of the material's orientation but at higher stretches the response in the muscle fibre direction is different from that in perpendicular direction.

#### 4. Viscoelasticity

Soft biological tissue shows elastic and viscous behaviour, that means that the loading and unloading curves do not coincide and you can see an open hysteresis loop in their load-deformation curves. This hysteresis correlates with the high water content but also with the presence of muscle.

### 5. Strain Rate Insensitivity

Soft tissue shows different properties under different strain rates, because of its viscoelastic behaviour. This means that higher strain rates give higher stresses. But this effect isn't very large in biological tissues, thus it is not very sensitive to strain rate.

### 6. Incompressibility

A water content of more than 70% (by wet weight) is responsible for the incompressible behaviour. Soft biological tissue hardly changes its volume even under load.

In summary, biomechanical characteristics result from the inner composition of the material, thus the microstructure is important to note. Furthermore, cells, tissues and organs in the cardiovascular system experience multiaxial states of stress, so we have to determine the multiaxial stress-strain behaviour, which is typically nonlinear, anisotropic over finite strains and inelastic [2, 18].

#### 1.2.2.2 Simple Shear

The mathematical representation of simple shear (deformation) is

$$x_1 = X_1 + \kappa X_2, \quad x_2 = X_2 \quad \text{and} \quad x_3 = X_3 \quad (1.1)$$

where  $(X_1, X_2, X_3)$  and  $(x_1, x_2, x_3)$  describe the Cartesian coordinates before respectively after deformation and  $\kappa > 0$  is called the amount of shear, a dimensionless constant. Shear is normally interpreted as two-dimensional. A rectangular specimen with dimensions that are all of the same order is deformed into a parallelogram [19], see Fig. 1.5.

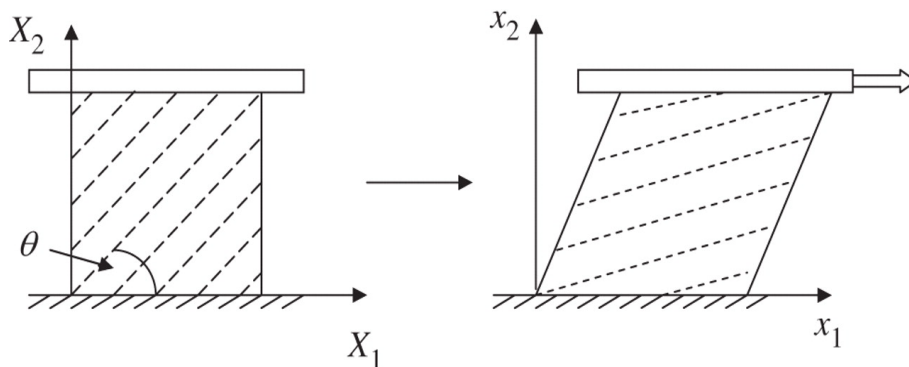


Figure 1.5: Simple shear of a specimen. Sketch adapted from [19].

The deformation gradient tensor  $\mathbf{F}$  for simple shear (1.1) is given by

$$[\mathbf{F}] = \begin{bmatrix} 1 & \kappa & 0 \\ 0 & 1 & 0 \\ 0 & 0 & 1 \end{bmatrix} \quad (1.2)$$

And the left Cauchy-Green strain tensor  $\mathbf{B}=\mathbf{F}\mathbf{F}^T$  can be described as

$$[\mathbf{B}] = \begin{bmatrix} 1 + \kappa^2 & \kappa & 0 \\ \kappa & 1 & 0 \\ 0 & 0 & 1 \end{bmatrix} \quad (1.3)$$

A typical tissue specimen has the following microstructural FSN coordinates according to [20]

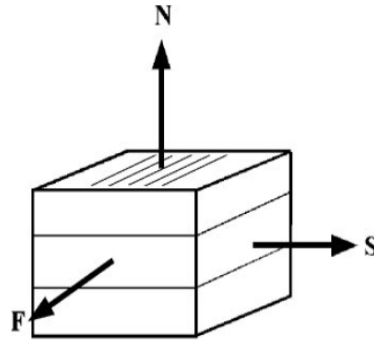


Figure 1.6: Sketch of the FSN coordinates of a tissue specimen adapted from [20].

$F$  is the direction of the myocytes,  $S$  lies within the muscle layer transverse to  $F$ , and  $N$  is normal to the muscle layer.

Six modes of simple shear are possible and to consider. To derive the Green strain tensor we will use the NS-mode as an example. We will use the following:  $X_1, X_2, X_3 = F, S, N$ ,  $x_1, x_2, x_3 = f, s, n$ , and the NS-mode presents the displacement of the N-face in the S-direction. A specimen  $P(F, S, N)$  is deformed into  $p(f, s, n)$  and  $k$  marks the shear deformation

$$f = F, \quad s = S + kN, \quad n = N \quad (1.4)$$

The deformation tensor  $\mathbf{F}$  is given by

$$[\mathbf{F}] = \begin{bmatrix} 1 & 0 & 0 \\ 0 & 1 & k \\ 0 & 0 & 1 \end{bmatrix} \quad (1.5)$$

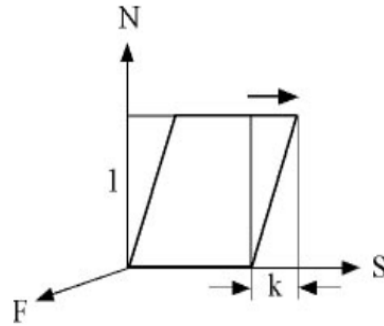


Figure 1.7: Simple shear of a block. Taken from [20]

The right Cauchy-Green tensor  $\mathbf{C}=\mathbf{F}\mathbf{F}^T$  can be described as

$$[\mathbf{C}] = \begin{bmatrix} 1 & 0 & 0 \\ 0 & 1 & k \\ 0 & k & k^2 + 1 \end{bmatrix} \quad (1.6)$$

And the Green strain tensor  $\mathbf{E}$

$$[\mathbf{E}] = 0.5(\mathbf{C} - \mathbf{I}) \quad (1.7)$$

Thus, the NS-mode is

$$[\mathbf{E}] = \begin{bmatrix} 0 & 0 & 0 \\ 0 & 0 & 0.5k \\ 0 & 0.5k & 0.5k^2 \end{bmatrix} \quad (1.8)$$

For the rest of the remaining shear modes the Green strain tensor is

NF-mode

$$[\mathbf{E}] = \begin{bmatrix} 0 & 0 & 0.5k \\ 0 & 0 & 0 \\ 0.5k & 0 & 0.5k^2 \end{bmatrix} \quad (1.9)$$

SN-mode

$$[\mathbf{E}] = \begin{bmatrix} 0 & 0 & 0 \\ 0 & 0.5k^2 & 0.5k \\ 0 & 0.5k & 0 \end{bmatrix} \quad (1.10)$$

SF-mode

$$[\mathbf{E}] = \begin{bmatrix} 0 & 0.5k & 0 \\ 0.5k & 0.5k^2 & 0 \\ 0 & 0 & 0 \end{bmatrix} \quad (1.11)$$

FN-mode

$$[\mathbf{E}] = \begin{bmatrix} 0.5k^2 & 0 & 0.5k \\ 0 & 0 & 0 \\ 0.5k & 0 & 0 \end{bmatrix} \quad (1.12)$$

FS-mode

$$[\mathbf{E}] = \begin{bmatrix} 0.5k^2 & 0.5k & 0 \\ 0.5k & 0 & 0 \\ 0 & 0 & 0 \end{bmatrix} \quad (1.13)$$



## 2 Materials & Methods

This section gives an overview of the experimental part of this thesis. From the material, thus the heart, to the methods with the myocardium sample preparation, the shear test device, the shear testing itself and the data analysis.

### 2.1 Materials

In this thesis exclusively human heart tissue was used, to be more precise the tissue of eleven different human hearts (mostly only parts of the heart due to the high demand for human tissue) were tested. All these hearts were provided by the Department of Transplantation Surgery, Medical University Graz.

Most of these hearts were non-failing from brain death patients, so the heart was in good condition but not suitable for transplantation due to different factors (age, diseases, alcohol, etc.).

The samples itself varied in shape and condition. Some of them were whole hearts (HH#28 and HH#29), while others were just a small part of the left ventricular free wall (LVFW), some where fresh (HH#29  $LV_1$ ), while others were frozen. Table 2.1 shows a listing of the tested hearts.

Table 2.1: Patient related heart data

Internal heart index	age (yrs)	sex	BMI (kg/m <sup>2</sup> )
#27	75	m	25
#28	43	m	24
#29	60	m	25
#30	74	m	25
#31	78	m	26
#32	73	f	-
#35	64	m	25
#36	-	-	-
#37	60	f	-
#39	-	-	-
#40	-	-	-

### 2.1.1 Collection and Storage of Materials

As we said above the samples were provided by the Department of Transplantation Surgery, Medical University Graz. Most of the samples were frozen already when they were received, so a cooling box was used (to prevent defrosting) to carry the heart samples from the LKH Graz to the laboratory of the Institute of Biomechanics where they were stored in a freezer ( $-25^{\circ}\text{C}$ ) until testing. Fresh samples lay in a cardioplegic solution and were also carried in a cooling box to keep the tissue cool. In the laboratory the samples were then tested immediately after the collection or they were frozen as well. Before testing the sample lying in cardioplegic solution was defrosted in the fridge over night to keep the tissue cool and wet during the whole experiment.

### 2.1.2 Solution for Storage and Testing

The heart tissue has to lie in solution during the whole time of the experiment. First of all to prevent tissue-drying and second to keep the tissue in a certain condition. And for this purpose different chemical solutions and agents were used depending on their field of application.

#### 2.1.2.1 Cardioplegic Solution (CPS)

To understand the mechanism of the cardioplegic solution let us first have a look at the membrane potential of a myocyte.

##### *General*

Cardiac cells have an electric potential across the cell membrane. This resting membrane potential can be measured and is determined by the concentration of positively and negatively charged ions ( $\text{Na}^+$ ,  $\text{K}^+$  and  $\text{Ca}^{++}$ ) across the membrane, the permeability of the membrane to the ions and the ionic pumps that transport these ions.  $\text{K}^+$ , which concentration in cardiac cells is high inside and low outside, is the most important ion to define the potential. Thus, a gradient exists and  $\text{K}^+$  diffuses out of the cell. On the contrary,  $\text{Na}^+$  and  $\text{Ca}^{++}$  have a gradient that runs in the opposite direction. Potassium runs out of the cell and the cell becomes more negative, which leads to a separation of charge and a potential difference across the membrane (negative inside relative to outside of the cell).

According to the Nernst potential the resting membrane potential is approximately  $-90\text{mV}$ .

$$E_{\text{K}} = -61 \log \frac{[\text{K}]_{\text{i}}}{[\text{K}]_{\text{o}}} = -96\text{mV} \quad (2.1)$$

in which  $[\text{K}^+]_{\text{i}}$  is  $150\text{mM}$  and  $[\text{K}^+]_{\text{o}}$  is  $4\text{mM}$ . So if the  $\text{K}^+$  concentration outside the cell increased the diffusion (from inside to outside) would be reduced; therefore, the membrane potential would be less negative [21].

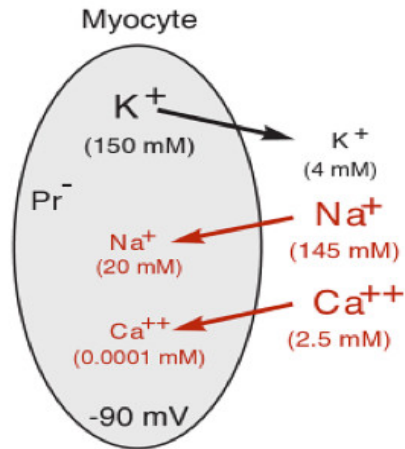


Figure 2.1:  $K^+$ ,  $Ca^{++}$  and  $Na^+$  concentrations of a cardiac myocyte at a potential of  $-90\text{mV}$  (resting membrane potential). Adapted from [21].

Cardioplegic solution is normally used to cause an artificial reversible cardioplegia, a cardiac arrest. This is necessary for most cardiac surgeries so that surgical procedures can be done in a still and bloodless field. Due to the application of CPS the electrical stimulus interrupts and with that the mechanical activity of the heart. Now the contraction is inhibited [22]. The oxygen demand in the resting myocardium is reduced, so the tolerance of ischemia is multiplied and the ischemic myocardium is protected from cell death [23, 24].

Cardioplegic solutions contain potassium and in high concentrations it decreases the membrane resting potential of ventricular myocardial cells. Extracellular CPS influences the membrane voltage, it becomes less negative and the cell depolarizes more easily. The depolarization causes contraction but the potassium prevents repolarization. The resting potential is approximately  $-84\text{mV}$  at an extracellular  $K^+$  concentration of  $5.4\text{mmol/l}$ . Enhancing the  $K^+$  concentration to  $16.2\text{mmol/l}$  raises this potential to  $-60\text{mV}$  and the muscle fibers are no longer excitable. If a potential of  $-50\text{mV}$  is reached an arrest of cardiac activity is achieved.

To summarise very briefly, heart tissue has to lie in cardioplegic solution for the whole experiment to prevent cell death during ischemia.

### 2.1.2.2 BDM - 2,3-Butanedione Monoxime

For fresh (not frozen) myocardial tissue 2,3-butanedione monoxime (BDM) plays an important role. BDM is an agent that acts as a potent inhibitor of myosin proteins, or more precisely muscle myosin-II [25]. Myosin-II is a so-called motor protein and is indispensable for muscle contraction and is as an essential part in muscles in the conversion of chemical energy in force and motion involved [24]. Thus, BDM blocks the function of myosin-II by inhibiting muscle contraction and ATPase activity [26].

BDM is useful for the improvement in the storage of transplants in order to organ preser-

vation in addition to its use to prompt cardioplegic arrest and protection of cardiomyocytes [27]. Thus, it is a very useful tool to prolongate the duration of cardioplegia and to prevent cell necrosis.

It inhibits force in both skeletal and cardiac muscle and it uncouples excitation from contraction. Furthermore, it prevents the rate of cross-bridge attachment, which leads to the decrease of maximal force [28].

For the inactivation of fresh myocardial tissue 0,5g BDM was mixed with 100ml cardioplegic solution and the specimen to be investigated was inlayed over the whole time of the experiment.

### **2.1.2.3 Formaldehyde**

Formaldehyde 4% is widely used as an agent for tissue fixation in histology. It stops autolysis and rot of medical tissue samples and creates a long durability [24].

It was used to make the specimen durable for further microscopic and morphological observations. Therefore, the specimen was marked in a certain way (see section 2.2.3) to obtain the sheet and fibre orientation.

## 2.2 Methods

### 2.2.1 Myocardial Samples

This section deals with the myocardial samples, for this reason, the dissection of the heart and preparation of the cubic specimen and the corresponding tools. The dissection of the heart in this section is shown with human heart 29 (HH#29) as it was a whole heart. Furthermore, the FSN-coordinate system is declared and the correct alignment of the cubic specimen axes with this coordinate system is shown.

#### 2.2.1.1 Tools for Heart and Specimen Preparation

First the most important utensils for heart and specimen preparation are shown with a brief declaration.

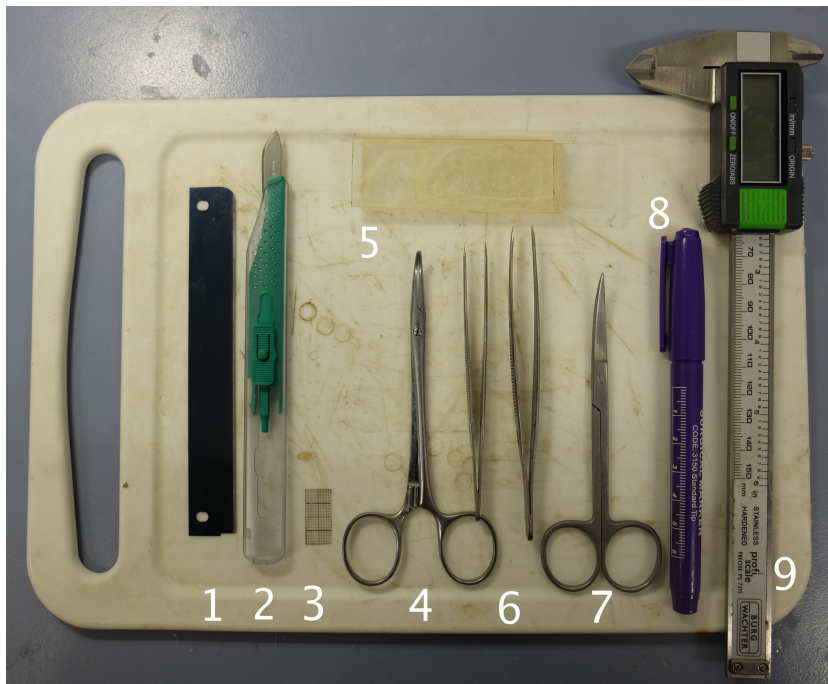


Figure 2.2: Tools for heart and specimen preparation

Explanation of tools according to Fig. 2.2:

1. dissection blade (very sharp) - good for straight cuts
2. surgical scalpel
3. plastic foil with mm-scale (like graph paper) - to measure the dimensions of the cubic specimens

4. surgical clamp - to fix the cubes (not to lose the correct alignment with the FSN-coordinate system)
5. selfmade tool - helps to prepare cubes with a good geometry
6. tweezers
7. surgical scissors
8. surgical marker - to mark the cubes after testing to define specimen orientation
9. caliper rule - to measure the size of the whole sample

### 2.2.1.2 Heart Dissection

This procedure is only necessary when the received sample is a whole heart. As already mentioned, human hearts 28 and 29 were received as a whole (see Fig. 2.3.(A)).

Before starting the work the heart sample was taken out of the freezer about 24 hours (for rather big tissue samples) before testing. It was put into the fridge at approximately 4°C for slow defrosting and to make sure that the tissue is always cooled.

The essential step in dissection is to separate the left ventricle and the septum. This is necessary because the actual specimens are mainly obtained from the left ventricle.

So first of all the upper part of the heart, the atrium, was cut off. As you can see by the dashed cutting line in Fig. 2.3. the cut shall be a bit higher than the equator of the heart and a precise cut is important to make sure not to cut off too much.

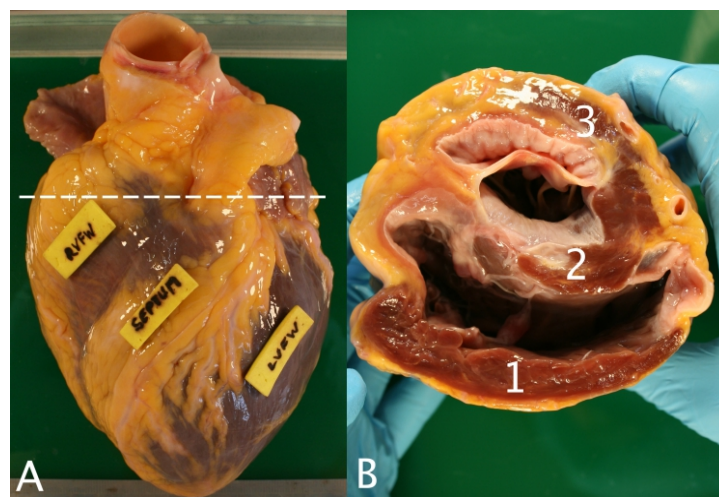


Figure 2.3: (A) shows the whole HH#29 with labeled right ventricle (RVFW), septum and left ventricle (LVFW) and an imaginary cutting line; (B) presents the inner heart with (1) the thin right ventricle, (2) the septum and (3) the thicker left ventricle



Now the right ventricle must be removed with a careful cut, as you can see in figure 2.4. The right ventricle is unusable for our purpose due to the fact that it is too thin for specimen preparation and the triaxial shear tests. It is very important to use a very sharp knife (e.g. a dissection blade) to carry out the cut precisely. If the right ventricle is thick enough it can be used for a test series (e.g. HH#29) As you can see in Fig. 2.4 (C) the septum and the left ventricle remain.

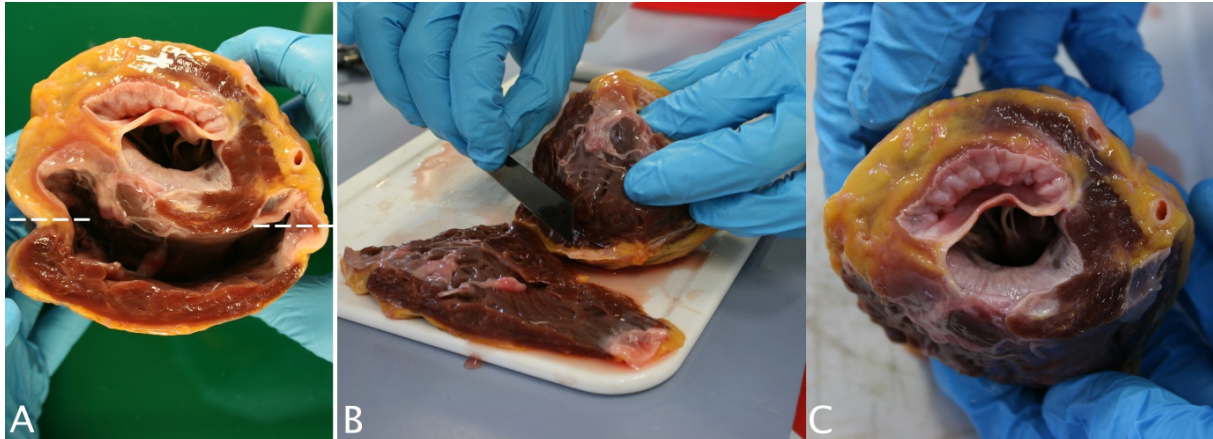


Figure 2.4: (A) shows the inner heart again, the lines demonstrate the cutting position of the right ventricle; in (B) the ventricle is already removed; (C) septum and left ventricle remain

The fragmentation of the septum and the left ventricle is now the last step of the dissection of the heart. In Fig. 2.5 you can see all parts of the heart separately, the septum and the left ventricle in (A) and the unusable right ventricle in (B). As mentioned in section 2.1.1 the heart tissue has to lie in cardioplegic solution and keep cool the whole time to prevent tissue dehydration and cell necrosis.

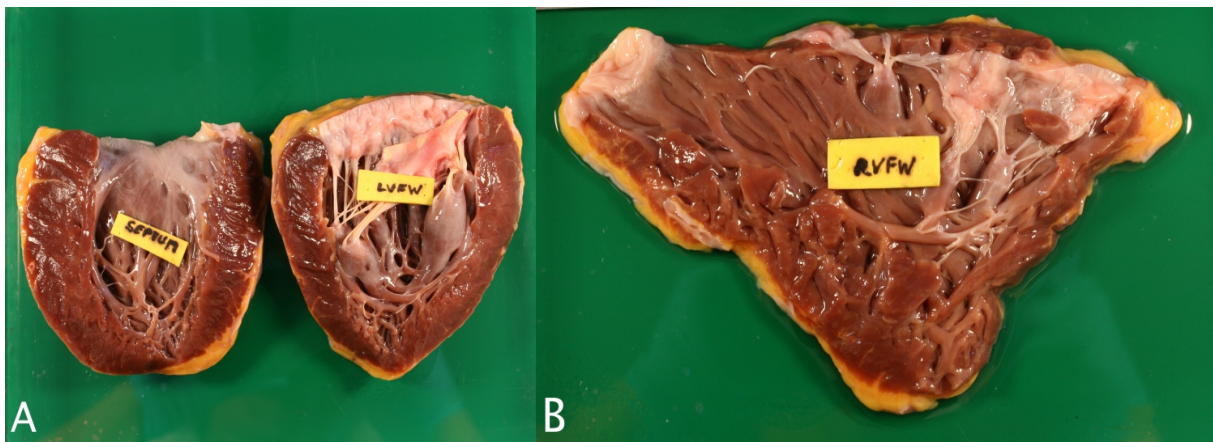


Figure 2.5: (A) shows septum and the left ventricle; (B) the right ventricle

After dissection of the heart the specimen preparation (cubic specimens) can start. Therefore, a certain coordinate system is used, the FSN-coordinate system which is explained in the next section.

### 2.2.1.3 Preparation of the Cubic Heart Specimens

This section deals with the correct cubic specimen preparation and the corresponding FNS-coordinate system.

The most important thing for an experiment is to get reconstructible and suitable data. In order to obtain this some guidelines are needed.

First of all a position within the heart should be defined where a slice is cut and it should be approximately the same for all specimens. That is limited by the size of the provided heart samples and so can not be maintained for all specimens. The position of the slices is either circumferential to the surface of the left ventricular free wall or perpendicular to the free wall, from epicardial to endocardial, as shown in Fig. 2.6 (B) (green coloured segments). Furthermore, a region should be selected in which the midwall muscle layers are most uniform in orientation to ensure a good alignment of sheets and fibers within the cube.

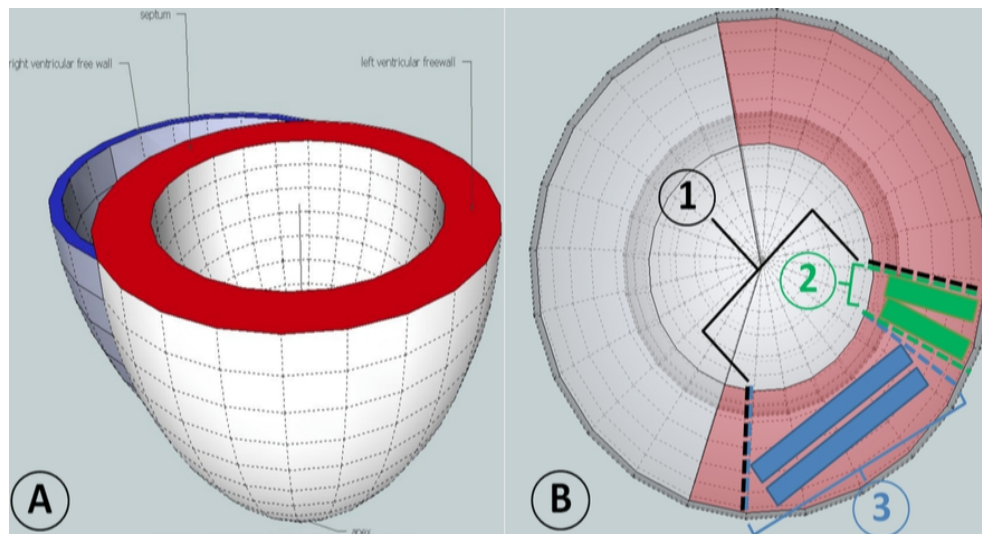


Figure 2.6: (A) shows a simplified 3D-model of a human heart with right ventricle, left ventricle and the septum; in (B) the area highlighted in red represents the left ventricle with cutting position for: (2) specimens for triaxial shear tests and (3) for corresponding biaxial tensile tests. Adapted from [29].

After the position of the slices within the tissue sample is found, the sheet and fiber orientation is very important. This step is the most challenging part of specimen preparation and for that purpose the FSN-coordinate system is needed.



### 2.2.1.4 The FSN-Coordinate System

This coordinate system is a right-handed orthogonal set of axes at every material point within the ventricular wall on the basis of the local laminar architecture. These axes match the main myofiber direction (F), the direction transverse to the fiber axis within the layer (S), and the direction normal to the layers (N), as shown in Fig. 2.7.

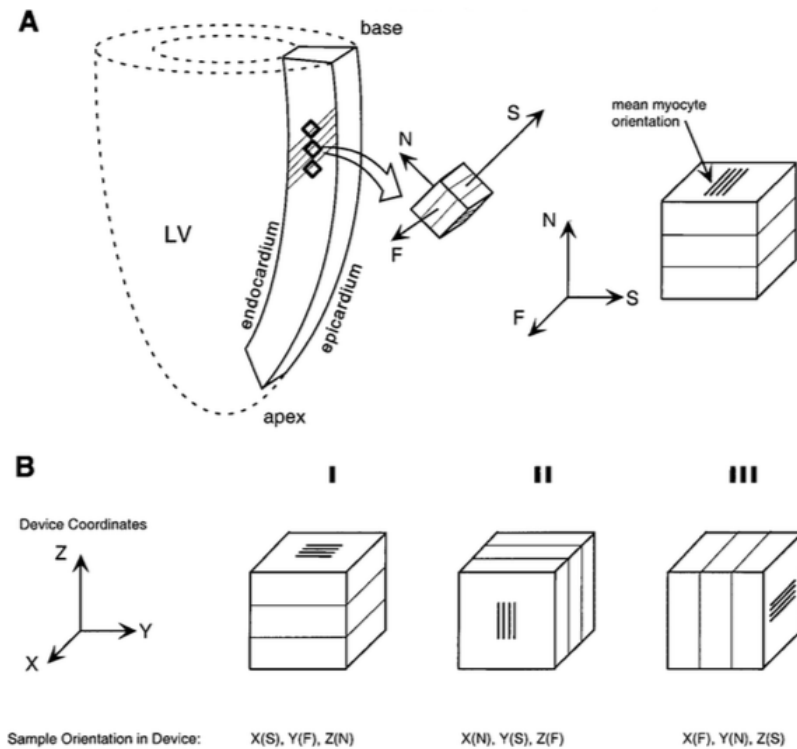


Figure 2.7: (A) shows the location and orientation of cubic samples within the heart and a transmural base-apex segment cut from the left ventricular (LV) free wall. (B) gives an example of sample orientations within the shear test device. Illustration adapted from [20].

Figure 2.8 shows the six possible modes of shear according to this FSN coordinate system. These six shear modes are very important to achieve an entire measurement series of an orthotropic material. Thus, three cubic specimens aligned with the FSN axes are needed to cover all six modes of simple shear [6]. So according to this three cubic specimens were prepared so that their edges were aligned with the laminae on the transmural face S and with two sides parallel to the F and N direction.

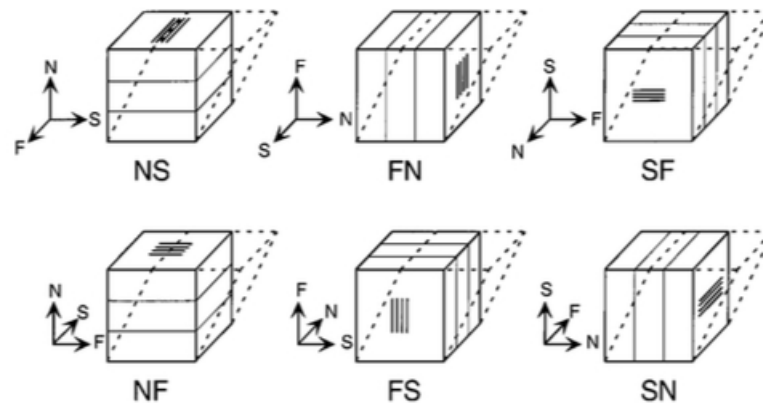


Figure 2.8: Six modes of simple shear according to the FSN coordinates. Shear deformation is characterized by two coordinate axes: one donates the face that is translated by the shear, and the other is the direction in which that face is shifted. Therefore, NS shear describes the translation of the N-face in the S-direction. Adapted from [20].

### 2.2.1.5 Preparation of three Cubic Specimens

As mentioned above three cubic specimens are needed to cover all six modes of simple shear. Further, these three cubes have to be aligned with the FNS-coordinate system. This means that the sheets and fibers have to lie in a certain way, see again Fig. 2.8. So the aim is to get three adjacent cubic blocks measuring  $3 \times 3 \times 3$  mm which edges are aligned with the laminae on the transmural face (S axis) and with two sides parallel to the F and N direction [20].

The first step was to cut a three millimeter thick slice of heart tissue within the sample in a region in which the sheet-layers are most uniform in orientation. Now the sheets are detected on this slice of tissue. Sheets are normally much easier to find than the fibers, because sheets consist of a few (four to six cells) cells and therefore have a better visible structure (broader layers). Outgoing from these sheets a  $3 \times 3 \times 3$  mm cubic block was prepared on which the orientation of the fiber was discovered. Finding the fibers is a very tricky task and requires a lot of concentration. At the end there should be a block like the one seen in Fig. 2.9 (B). If sheets and fibers do not lie in a perfect way the results will not be good (see section Results).

After preparation the exact dimensions of each myocardial block were measured (with plastic foil like graph paper) and noted down. Then the specimen had to be attached to the upper platform (stamp) of the testing device. For this a small drop of cyanoacrylate adhesive (super glue) was used. The glue was applied to the stamp, spread until it was a thin and uniform layer and then the cubic specimen was placed very carefully on the quadratic mark on the stamp. It is very important to place the specimen in the right way with the

correct sheet and fiber orientation. After that the specimen was gently pressed down for a few seconds to achieve a good adhesion. Then the sample was ready for inserting in the testing apparatus.

The waiting times between the individual steps have to be reduced to a minimum, because the tissue should lie in solution and this is not the case anymore. Thus, the next steps have to be performed very quickly.

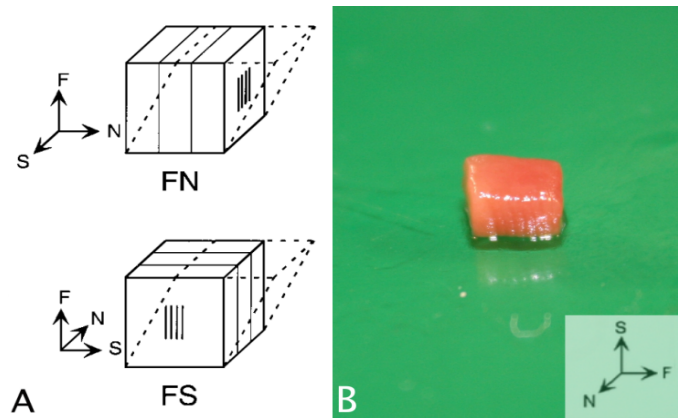


Figure 2.9: (A) shows a cubic block in FSFN mode. Adapted from [20]; (B) demonstrates the same cubic specimen with sheets on the front and fibers on the top.

FSFN-mode means in this case that the specimen is shifted first in  $x$ -direction (FS-mode: translation of the F-face in the S-direction) and then in the  $y$ -direction (FN-mode: translation of the F-face in the N-direction).

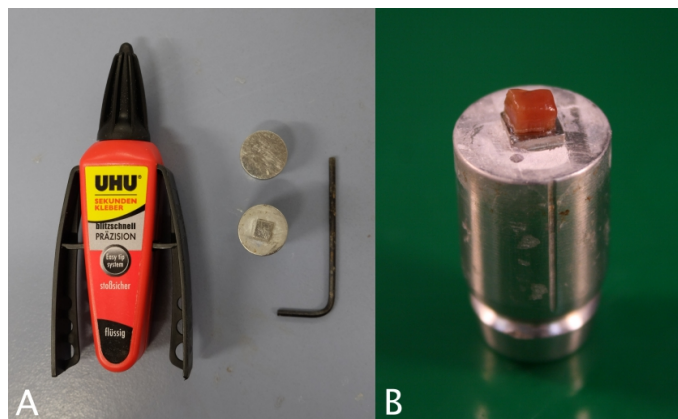


Figure 2.10: (A) Utensils for the fixation of the myocardial cube and (B) the cubic block attached to the upper platform (stamp) ready for inserting in the testing apparatus

## 2.2.2 Shear Test Device

This section deals with the triaxial shear testing device (quick: TRIAX) or rather with the setup and the functionality of it.

The shear testing device was developed, constructed and processed by the Institute of Biomechanics (Graz University of Technology, Austria) in cooperation with MESS-PHYSIK Materials Testing (Fuerstenfeld, Austria). Further, the device was optimized for testing soft biological tissue with high deformation under shear deformation [29].

### 2.2.2.1 Instruments

Figure 2.11 shows a block diagram of the whole experimental setup for the measurement of the properties of human myocardiums.

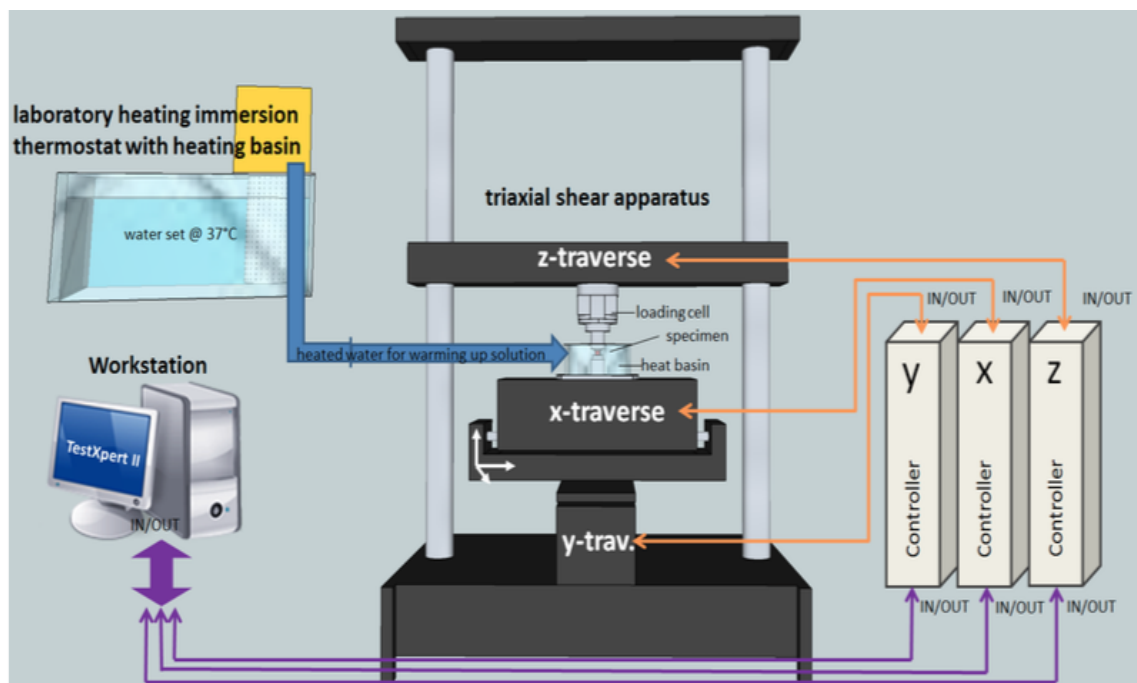


Figure 2.11: Block diagram of the experimental setup. Adapted from [29].

Declaration of instruments according to Fig. 2.11:

1. Workstation - Computer  
used as control monitor  
with TestXpert II software for programming, testing and data evaluation  
- ZWICK/ROELL GmbH & Co. KG, Germany
2. Triaxial shear apparatus - shear test device (TRIAX)  
with triaxial loading cell  
- MESSPHYSIK Laborgeräte GmbH, Austria

3. Three controlling towers  
connected to the testing device  
one for each direction: X -, Y-, and Z-traverse  
- ZWICK/ROELL GmbH & Co. KG, Germany
4. Heating thermostat with basin  
to simulate the physiological environment of the specimen

### 2.2.2.2 Setup of the Triaxial Shear Test Device

Figure 2.12 shows a photograph of the experimental setup of the shear testing device which is located in the Institute of Biomechanics, Graz University of Technology.

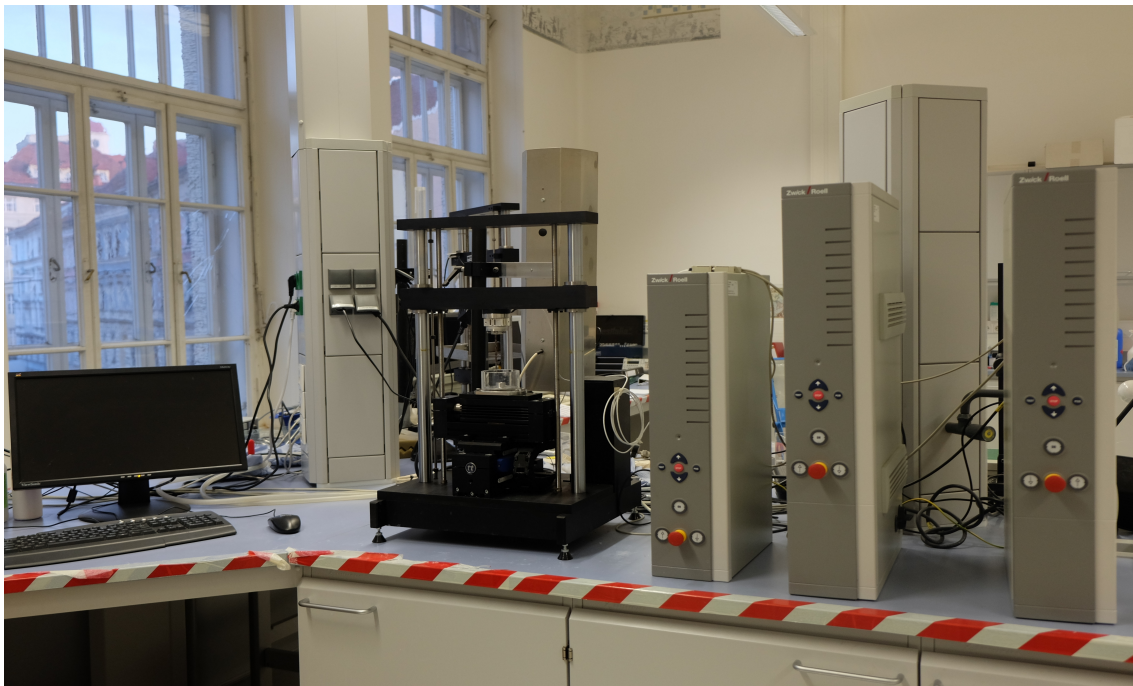


Figure 2.12: Triaxial shear testing device (middle) with the computer (rleft) and three controlling towers (Z, Y, X) (right).

The measuring apparatus consists of different devices. The core components are the shear testing device itself with its three controlling towers.

The functional principle is based on three traverses, which can be moved in X-, Y- and/or Z-direction. The device consists of separate X-, Y- and Z-translation stages attached to fixed bases, the upper and the lower platform. The X-traverse (movement in  $x$ -direction) is attached to the Y-traverse (movement in  $y$ -direction) which is located on the lower platform. In contrast the Z-traverse (movement in  $z$ -direction) is attached to the upper platform and

the bars on each side, shown in Figs. 2.11, 2.12 and 2.13. Each traverse is connected to its own controlling tower. These towers are controllable either manually with buttons on the front side of the towers or via the computer. To control the three towers and thus the individual traverses the software TestXPertII is used, which also is used for data evaluation. Thereby, the lower platform is moved relative to the fixed upper platform and operates with a stroke resolution of  $0.04 \mu\text{m}$  in  $z$ -direction and of  $0.25 \mu\text{m}$  in  $x$ - and  $y$ -direction.

Furthermore, the triaxial loading cell (3-axes force-sensor) which is located on the  $Z$ -traverse plays an important role. It allows the three orthogonal forces in all directions ( $x$ -,  $y$ - and  $z$ -direction) to be recorded. The maximum values are of particular importance. They are not allowed to exceed a specific value because of the risk of injury or damage of the apparatus. The nominal maximal force for all three directions is  $\pm 2\text{N}$  according to the manufacturer.

A small tissue bath assembly is located on the  $X$ - $Y$  translation stage (lower platform) in which a small stamp can be fixed in the middle. To this stamp the specimen is attached during testing. The basin is filled with a specific solution, see section 2.1.2, and is tempered (approx.  $37^\circ\text{C}$ ) to simulate the physiological environment of the specimen. On the upper platform the counterpart of the stamp is located to fix the specimen from above, as seen in Fig. 2.13 (B). So the tissue specimen is positioned between two circular platforms within this tissue bath [30].

To carry out the shear test, the bottom of the tissue specimen is shifted horizontally with the help of the  $X$ - $Y$  translation stage (see Fig. 2.13 (B)), while the appropriate forces in three orthogonal directions ( $x$ -,  $y$ - and  $z$ -direction) are measured.

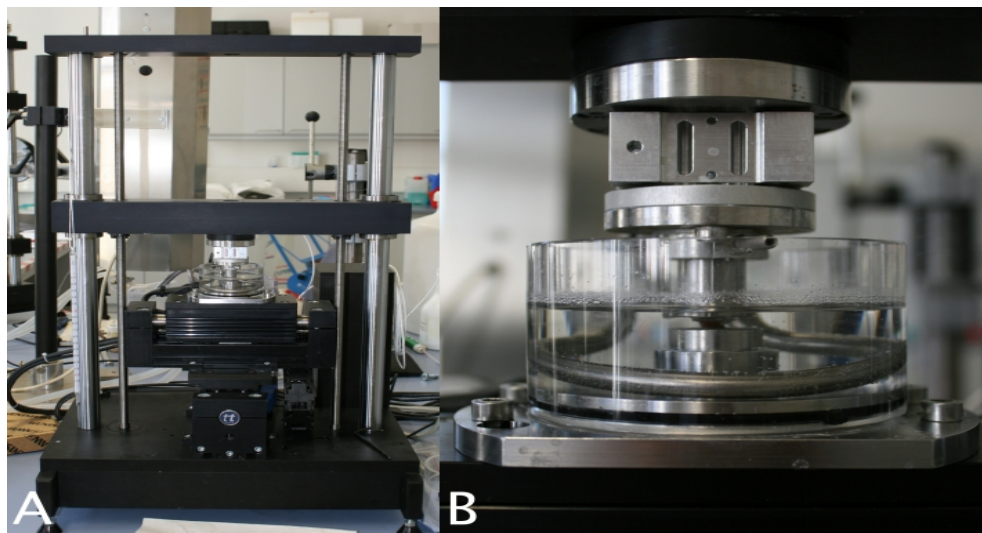


Figure 2.13: (A) shows the shear test device (TRIAX) and (B) the tissue bath filled with cardaplegic solution and a cubic specimen fixed between the upper and lower stamp

### 2.2.3 Shear Testing

Before testing you have to make sure that the testing apparatus is ready for testing and for this a few steps have to be carried out.

Process for initializing the shear testing device:

1. Heating tank

- Turn on the heating tank, fill it with water and set the temperature to 41°C to ensure that the temperature of the tissue bath is 37°C. The heat loss can be explained through the long tubes.

2. X-Y translation stage (lower platform)

- Before starting the test protocol ensure that the X-Y translation stage is in a certain position (pulled all the way to the front and to the right). Otherwise it is not possible to fix the specimen correctly (upper and lower platform are positioned against each other).

3. Hardware and software

- Turn on the computer and the three controlling towers (on the back side of them). Then start the software TestXPertII.

4. Controlling towers

- Press the "ON" buttons on the controlling towers to activate them.
- Click on "Maschine" and set the first two position parameters ("Aktueller Werkzeugabstand/ aktuelle Einspannlänge") to 0 and click on "Kräfte Nullen".

This procedure has to be done every day before the very first test is started. For each further test the shear testing device is initialized after that and you can start the procedure from the next chapter downward.

#### 2.2.3.1 Fixation of Specimen into the Triaxial Shear Device

As seen in Fig. 2.10 one of three cubic specimens is prepared and fixed on the stamp ready for testing. Now the stamp has to be affixed onto the shear test device at the upper platform so that the specimen hangs upside down with the notch on the stamp forward (a mark is obvious on the upper platform as well). Now the shear test device and the test itself can be started.

### 2.2.3.2 Testing Protocol

After preparation and fixation of the specimen and the description of the experimental setup the testing procedure is described.

#### *Shear testing*

Start the testing procedure using TestXPertII. First of all the sample properties like trial name and the amount of shear (10 to 50%; to set always before starting a test cycle), have to be set, as seen in Fig. 2.14. For this go to “Assistent” (blue button on the top) and “Prüfparameter” in TestXPertII. After that the exact specimen dimensions must be specified under the point “Probendaten”, as you can see in Fig. 2.15. Now the shear tests can begin and the instructions of the software should be followed:

1. Apply adhesive - yes/no?

Choose yes for the first cycle (10% amount of shear) of each specimen otherwise the fixation of the already fixed specimen will be lost and also the specimen itself will be damaged and useless.

First apply adhesive to the lower stamp, spread it until it is a thin and uniform layer and position it on the X-Y translation stage in the provided spot. The final fixation of the specimen follows while the specimen is compressed between the lower and the upper platform with a load of 400–600 mN over a period of five minutes. This technique provides a high-strength bond in shear [20].

2. Fill in the solution and wait for temperature to be reached

After a few minutes of compression, the tissue bath is filled with solution (cardioplegic solution with or without BDM, depending on the tissue; see section 2.1.1) and a temperature of 37°C is waited for.

3. Start

Now the first cycle of simple shear with an amount of shear of 10% in  $x$ -direction is performed. The first two cycles are for preconditioning and the third cycle is for data recording and analysis.

Make sure that the waiting times between the different steps of testing are reduced to a minimum and that the tissue is always stored in solution and cooled. The specimen cubes tend to soak up the cardioplegic solution and lose their shape by and by.



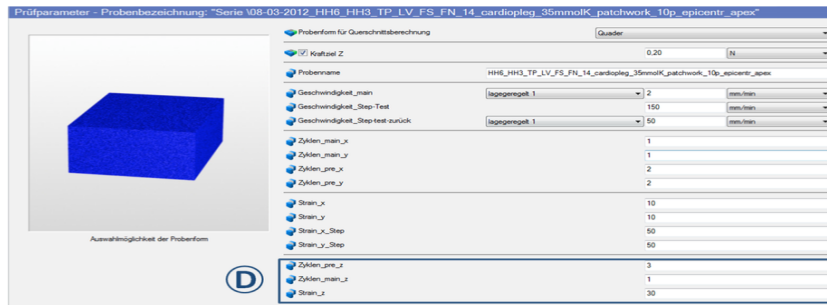


Figure 2.14: TestXPertII Layout-Assistant for setting the sample properties before testing

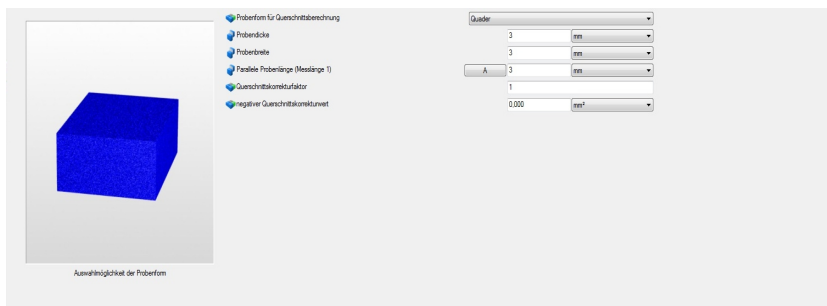


Figure 2.15: TestXPertII Layout-Assistant for setting the exact specimen dimensions before testing

Shear testing was performed under quasistatic conditions, that means that this process happens “infinitely slowly”. Such processes can be realized by performing them very slowly [24]. For each direction ( $x$ - and  $y$ -direction) three cycles of sinusoidal shear were carried out, the first two cycles for preconditioning because a tissue softening occurs and the third cycle for data recording and analysis. A sequence of tests is performed in which the maximum shear displacement is increased from 10, 20, 30, 40 and 50% of specimen thickness in two orthogonal directions,  $x$ -direction first and than  $y$ -direction. Shear displacement means a shift of the upper relative to the lower platform. For the existing six modes of simple shear three cubic specimen are needed.

During the test series the recording of the data can be observed via the software under the button “preconditioning”. In Fig. 2.16 four measuring curves can be seen. The first two (black curves) for  $x$ -direction and the second two (red curves) for  $y$ -direction, whereby preconditioning is presented by the first curves for the respective direction.

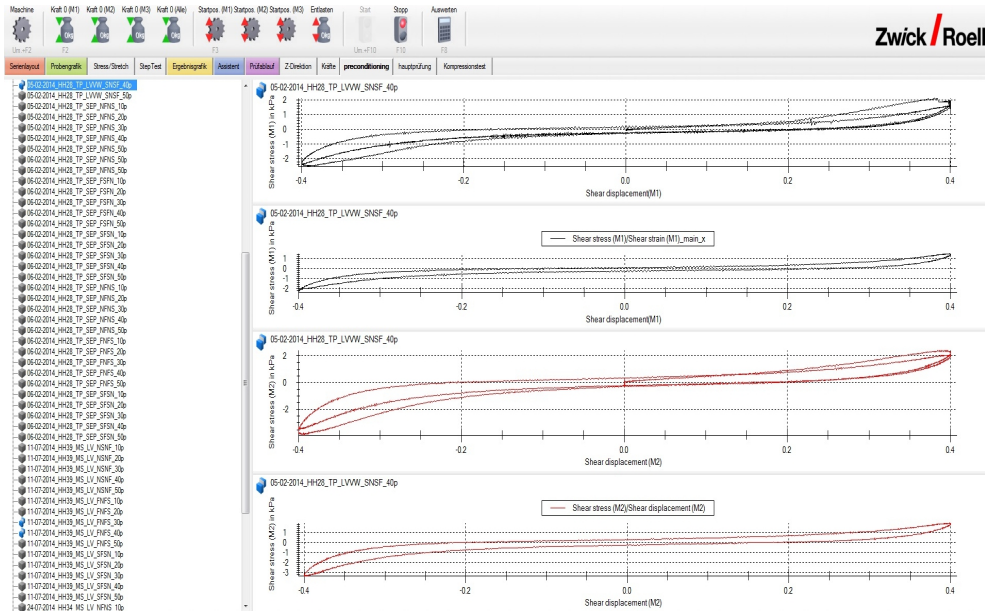


Figure 2.16: Preconditioning and data recording cycles of a typical sample

After testing the tissue bath is drained and the upper stress platform is manually brought into a higher position. The blocks are carefully removed from the apparatus and marked in a certain way (small dots on two specific corners), as you can see in Fig. 2.17. This marking is important to obtain the sheet and fiber orientation for the storage in formalin for further microscopic and morphological observations [20].

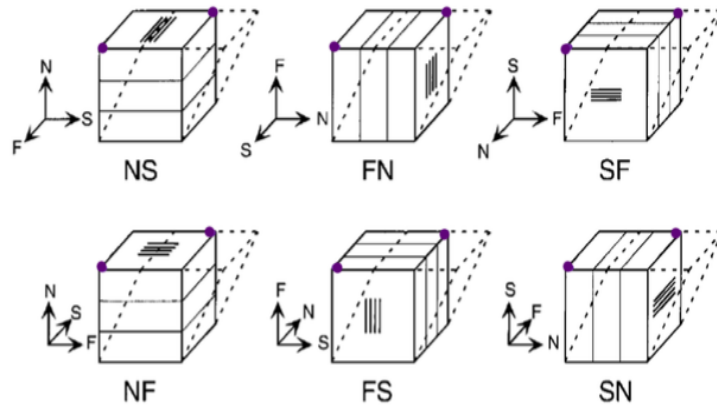


Figure 2.17: Three cubic specimens for six possible modes of simple shear with the correct marking (violet dots on the top) in two corners

After this whole procedure new cubic specimens can be prepared and the test cycle can be repeated.

## 2.2.4 Data Analysis

For the visualization and further interpretation of the recorded data a Matlab script was used. This script is realized as a Matlab®GUI (graphic user interface) and was developed by Franz Maier, Michael Kutschera and Christoph Schwarz.

### 2.2.4.1 MATLAB®Data Evaluation Script

Figure 2.18 shows the graphic user interface (GUI) of the Matlab script with its various options for data analysis:

1. Steptest - in X-,Y- or XY-directions
2. Original stress-strain curves - in X-,Y- or XY-directions
3. Stress-strain curves - in X-,Y- or XY-directions - with applied smoothing and offset corrections

The button “Stress Strain (xy) (Smooth+offset-corr.)” has the greatest significance to visualize the data. You can select one or more samples in the lower box and these files are processed and visualized at once. Further, a smoothing and offset-correction is applied on the plots.

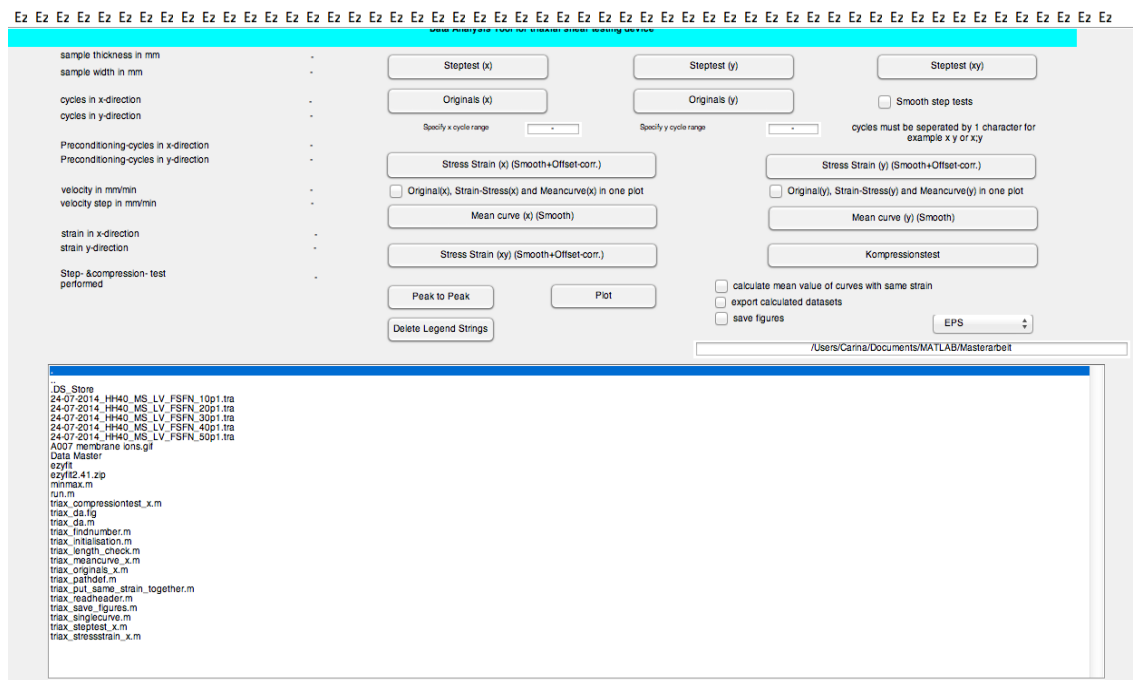


Figure 2.18: Overview of the MATLAB®GUI

The result is shown in Fig. 2.19, where you can see a plot of a typical shear stress-strain curve (FS-FN modes, from 10-50% shear displacement) within the Matlab editing interface.

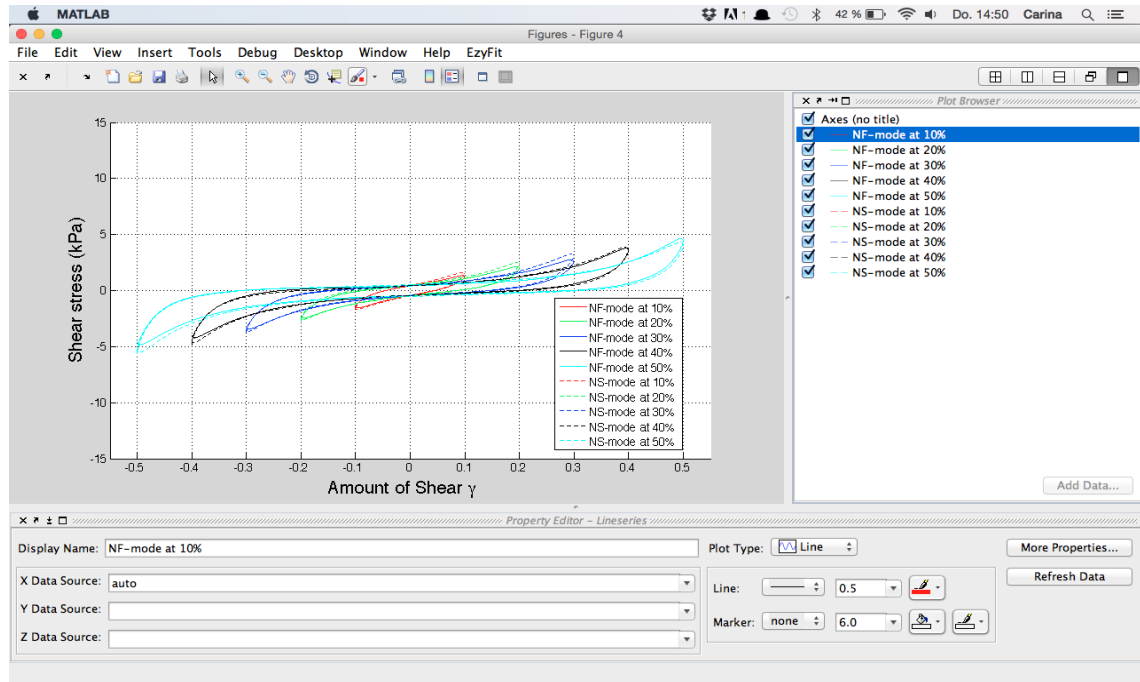


Figure 2.19: Plot of typical shear stress vs. amount of shear curves (FS- and FN-modes) within the MATLAB® editing interface

For an additional and detailed description of the several functions of the Matlab graphic user interface the reader is referred to Maier (2011).

### 3 Results

This section deals with the presentation of the results which are most relevant related to this thesis. The main aspect was to determine the triaxial shear properties of the myocardium and prospective the verification and possible modification of the novel structurally-based constitutive model of the passive human myocardium, as proposed by Holzapfel and Ogden in 2009 [6]. For this purpose 11 different hearts, 20 heart samples and in total over 60 cubic specimens were tested.

For each heart sample three cubic blocks were prepared to cover all six modes of simple shear (NF/NS, SF/SN, FS/FN). For all cubic blocks the test procedure was the same. Three sinusoidal cycles of simple shear, two for preconditioning and one for data analysis, with an increasing shear displacement from 10% to 50% (0.1-0.5 in 0.1 steps of specimen thickness). This occurred in two orthogonal directions, first in  $x$ -direction and then in  $y$ -direction.

The resulting data were then plotted as shear stress vs. amount of shear curves, as seen in Fig. 3.1. It shows a typical curve in NF/NS mode. The cycles of the testing sequence have an amplitude increasing in steps of 0.1 up to 0.5 shear displacement. These loops do not overlay each other with increasing shear strain amplitudes. Same effects can be seen for the two other modes (FS/FN and SF/SN) but with higher and reduced stress amplitudes for the same deformation, respectively. The two preconditioning cycles are not shown on the plots, but showed higher stress levels in both directions, meaning a stiffer behavior.

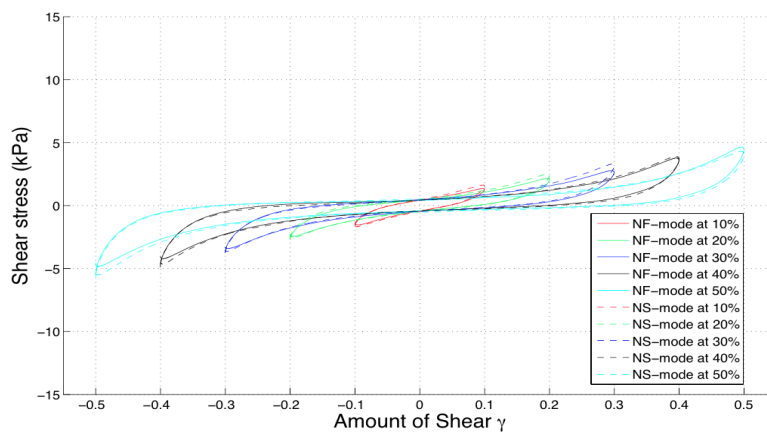


Figure 3.1: Relationship of shear stress and amount of shear during testing cycles of sinusoidal simple shear in NF/NS mode. Maximum amount of shear is increased from 0.1 to 0.5.

### 3.1 Results of the Shear Test

Table 3.1 gives a rough overview of relevant information of the tested heart specimens with regard to the shear test. That includes the tested location (LV...left ventricle, RV...right ventricle, Sep...septum), the dimensions of the cubic specimens, which are very important for the shear testing itself (amount of shear is based on the specimen thickness), the used solution in the tissue bath and the shear mode.

Table 3.1: Overview of relevant information of the tested heart specimens with regard to the shear test

Internal heart index	Location tested	Dimensions $w \times l \times h$ (mm)	Solution	Shear mode
#27	LV <sub>1</sub>	3 × 3 × 4	CPS	NF/NS
		3 × 3 × 2	CPS	FN/FS
		5 × 4 × 4	CPS	SF/SN
	LV <sub>2</sub>	4 × 3 × 4	CPS	NF/NS
		3 × 3 × 3	CPS	FN/FS
		4 × 4 × 4	CPS	SN/SF
#28	LV <sub>1</sub>	3 × 3 × 3	CPS	NF/NS
		4 × 4 × 4	CPS	FS/FN
		3 × 3 × 3	CPS	SN/SF
	LV <sub>2</sub>	3 × 3 × 3	CPS	NF/NS
		4 × 4 × 4	CPS	FS/FN
		4 × 3 × 4	CPS	SN/SF
	Sep <sub>1</sub>	4 × 4 × 3	CPS	NF/NS
		5 × 5 × 6	CPS	FS/FN
		5 × 4 × 5	CPS	SF/SN
	Sep <sub>2</sub>	5 × 5 × 5	CPS	NF/NS
		4 × 4 × 4	CPS	FN/FS
		4 × 4 × 4	CPS	SF/SN
#29	LV <sub>1 fresh</sub>	3 × 3 × 3	CPS+BDM	NF/NS
		4 × 3 × 4	CPS	FN/FS
		4 × 4 × 4	CPS	SF/SN
	LV <sub>2</sub>	4 × 4 × 4	CPS	NF/NS
		3 × 3 × 3	CPS	FN/FS
		4 × 3 × 3	CPS	SF/SN
	Sep <sub>1</sub>	3 × 3.5 × 3.5	CPS	NF/NS
		3 × 3 × 3	CPS	FN/FS
		4 × 4 × 5.5	CPS	SN/SF
	Sep <sub>2</sub>	3 × 3 × 3	CPS	NF/NS
		4 × 4 × 4	CPS	FN/FS
		3 × 4 × 3	CPS	SF/SN

Table 3.1: Overview: Continuation

Internal heart index	Location tested	Dimensions $w \times l \times h$ (mm)	Solution	Shear mode
	RV	$4 \times 5 \times 3$	CPS	NF/NS
		$3 \times 3 \times 3$	CPS	FN/FS
		$3 \times 3 \times 3$	CPS	SF/SN
#30	LV	$3.5 \times 4 \times 3$	CPS	NF/NS
		$3 \times 4 \times 3$	CPS	FS/FN
		$3 \times 3 \times 3$	CPS	SN/SF
#31	LV	$3 \times 3 \times 4$	CPS	NF/NS
		$3.5 \times 3 \times 3$	CPS	FS/FN
		$4 \times 3 \times 4$	CPS	SN/SF
#32	LV	$3 \times 4 \times 3$	CPS	NF/NS
		$4 \times 4 \times 4$	CPS	FS/FN
		$3 \times 3 \times 4$	CPS	SN/SF
#35	LV	$3 \times 4 \times 2$	CPS	NS/NF
		$4 \times 4 \times 4$	CPS	FS/FN
		$3 \times 3 \times 3$	CPS	SF/SN
	Sep	$3 \times 3 \times 3$	CPS	NF/NS
		$3 \times 4 \times 3$	CPS	FS/FN
		$3 \times 4 \times 4$	CPS	SF/SN
#36	LV	$4 \times 4 \times 4$	CPS	NS/NF
		$3.5 \times 4.5 \times 4$	CPS	FN/FS
		$3.5 \times 4 \times 3.5$	CPS	SF/SN
#37	Sep	$3.5 \times 4 \times 3$	CPS	NS/NF
		$4 \times 4 \times 4$	CPS	FS/FN
		$4 \times 4 \times 4$	CPS	SF/SN
#39	LV	$5 \times 5 \times 5$	CPS	NS/NF
		$3 \times 3 \times 3$	CPS	FN/FS
		$4 \times 4 \times 5$	CPS	SF/SN
#40	LV	$4.5 \times 4 \times 4$	CPS	NF/NS
		$5 \times 5 \times 5$	CPS	FS/FN
		$4 \times 4 \times 4$	CPS	SF/SN

In total eleven different hearts (mostly only parts of the organs due to the high demand for human tissue) from the Department of Transplant Surgery (Medical University, Graz) were examined. They were all in a passive state due to inactivation of the tissue. Most of the hearts were frozen, some of them over a longer period of time which we don't know exactly. The freezing results in a change of properties in the tissue. Already during dissection of the heart and preparation of the cubic specimens it was noticed that the tissue got softer.

All in all it was difficult to prepare good cubic specimen. They were mostly larger in size (more than 3 mm edge length) and the preparation of an acceptable cube geometry was challenging. A comparison of results with non-frozen samples is unfortunately not possible due to the fact that there was just one opportunity to test a fresh tissue sample during this thesis.

Although the specimens were cut from nearly the same region, where the fiber orientation does not change steeply, the direction of the sheets on both of the surfaces (on the opposite side of the cubic specimen) was not the same. That indicates that there is a change in the fiber orientation up to  $30^\circ$  across each block [20]. Thus, the alignment to the FSN-coordinate system was very hard and not guaranteed for all specimens due to change in fiber orientation, inhomogeneities and fat inclusions in the human heart tissue.

Shear stress was always greater in the first few cycles of shear in positive and negative direction than in subsequent cycles. After one cycle of sinusoidal shear the shear stress vs. amount of shear loops did not change anymore, they were reproducible. This softening was seen in  $x$ - and  $y$ -direction [20].

Furthermore, the shear properties of the human myocardium were nonlinear, viscoelastic and anisotropic. Anisotropic means that the properties are highly dependent on the orientation of the myofibers and sheets within the cardiac tissue, which shows the orthotropic nature of myocardial tissue [6].

As already known six modes of simple shear (FS, FN, SF, SN, NF and NS) exist, whereby the FN- and FS-modes show higher shear stresses at equivalent amount of shear than the four other modes. This is observed in most of the experiments with good data. It indicates that the shear properties are significantly anisotropic, with the highest resistance to shear in FS- and FN-modes, intermediate in SF- and SN-modes and the lowest in NS- and NF-modes. Thus, there is a significant difference in the shear stress-amount of shear relationship for all three pairs of directions (FSFN > SFSN > NFNS). But there are no differences within the three pairs, so FN is not different from FS and so on.

Figures 3.2, 3.3 and 3.4 show representative results of shear stress-amount of shear relationships of the three different parts of the heart. The left and the right ventricle and the septum, can be seen. The shear stress vs. amount of shear curves are to some degree symmetric. This is very important, otherwise the obtained data is not good. But it is very difficult to get completely symmetric curves due to the correct alignment with the FSN-coordinate system. The order of the stiffness of the different shear modes (FSFN > SFSN > NFNS) is correct as well.



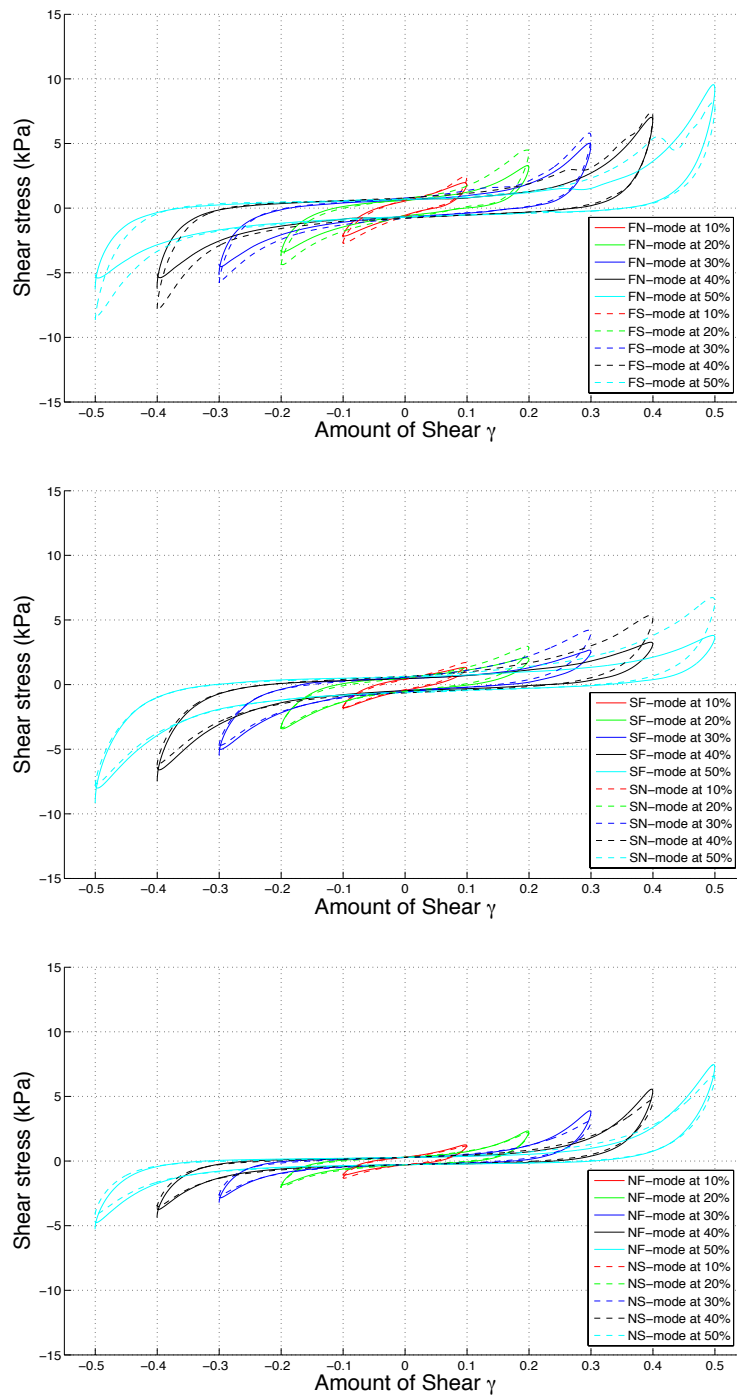


Figure 3.2: Shear stress vs. amount of shear curve of a left ventricle (HH#29) in FN/FS (top), SF/SN (middle) and NF/NS mode (bottom) increasing from 10% to 50%.

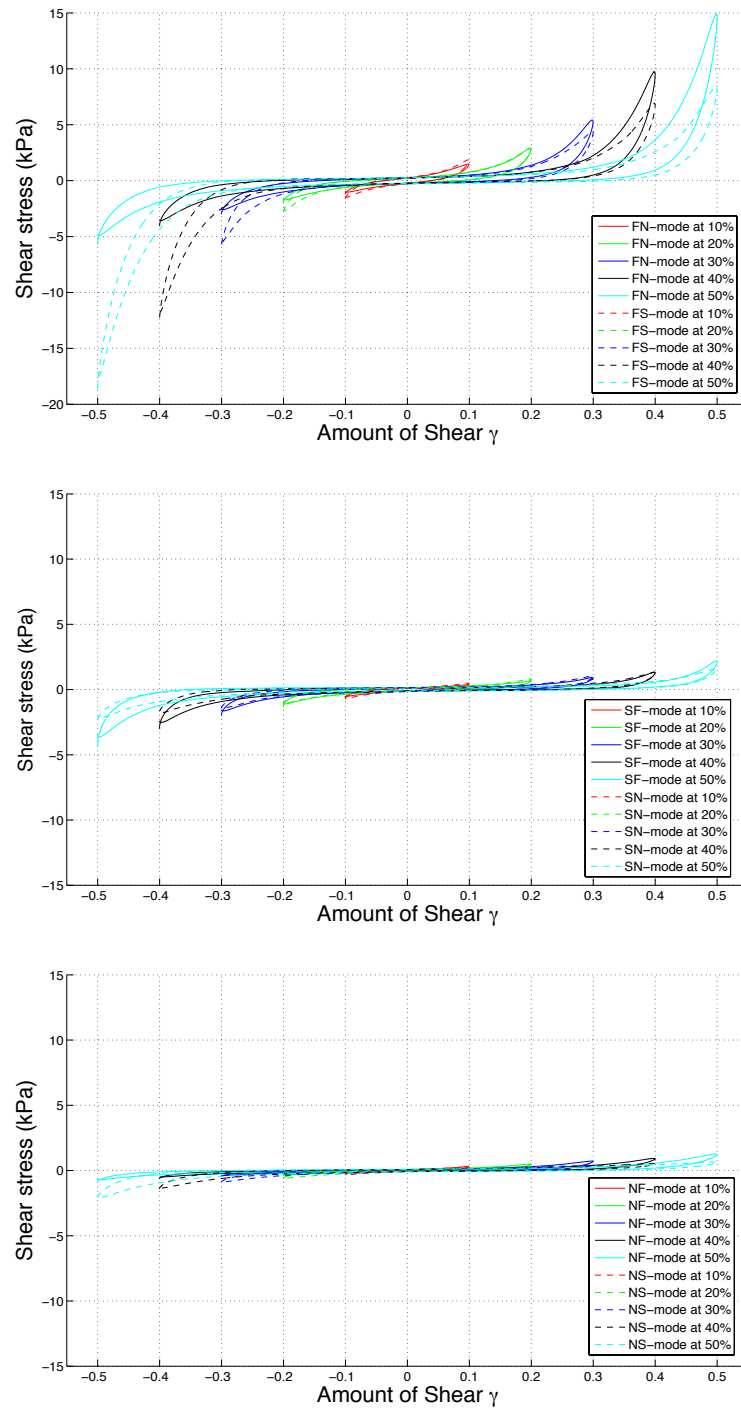


Figure 3.3: Shear stress vs. amount of shear curve of a right ventricle (HH#29) in FN/FS (top), SF/SN (middle) and NF/NS mode (bottom) increasing from 10% to 50%.

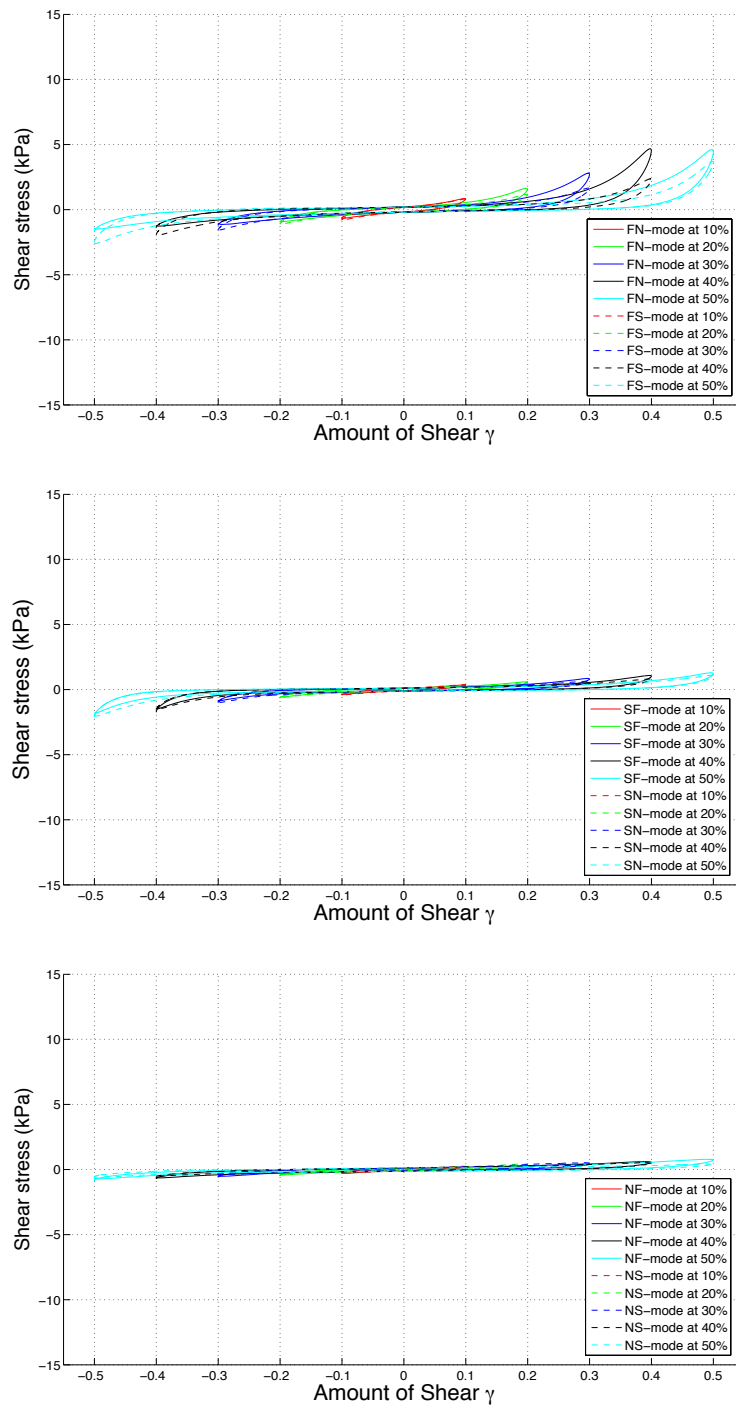


Figure 3.4: Shear stress vs. amount of shear curve of a septum (HH#28) in FN/FS (top), SF/SN (middle) and NF/NS mode (bottom) increasing from 10% to 50%.

## 3.2 Example of Failed Testing

The accurate alignment of fibers and sheets with the FSN-coordinate system and the fixation of the specimen in the shear testing device is of critical importance. If this work is done improperly the resulting data is poor. That means that the shear stress vs. amount of shear curves are very asymmetric or the test fails on the whole.

The alignment with the coordinate system is the most challenging part of the whole work. Fibers and sheets are more or less difficult to define, depending on the condition of the tissue. Furthermore, as described above in section “Analysis of the heart” the alignment was not guaranteed for all samples due to change in fiber orientation (although the specimen were cut from nearly the same region the direction of the sheets was not the same), inhomogeneities and fat inclusions in the human heart tissue. In such cases the shear stress vs. amount of shear curves become asymmetric. Tests that resulted in such or comparable data were either repeated, if it was possible, or disregarded.

Figure 3.5 shows a tested left ventricle from human heart 32 (HH#32) with a failed NF/NS mode (undermost shear stress vs. amount of shear curve). In this case the specimen was badly affixed to the upper stamp and the fixation dissolved at an amount of shear of 30% in y-direction. Because the received piece of myocardial tissue was very small the NF/NS mode could not be repeated so HH#32 was rejected for the statistical analysis.

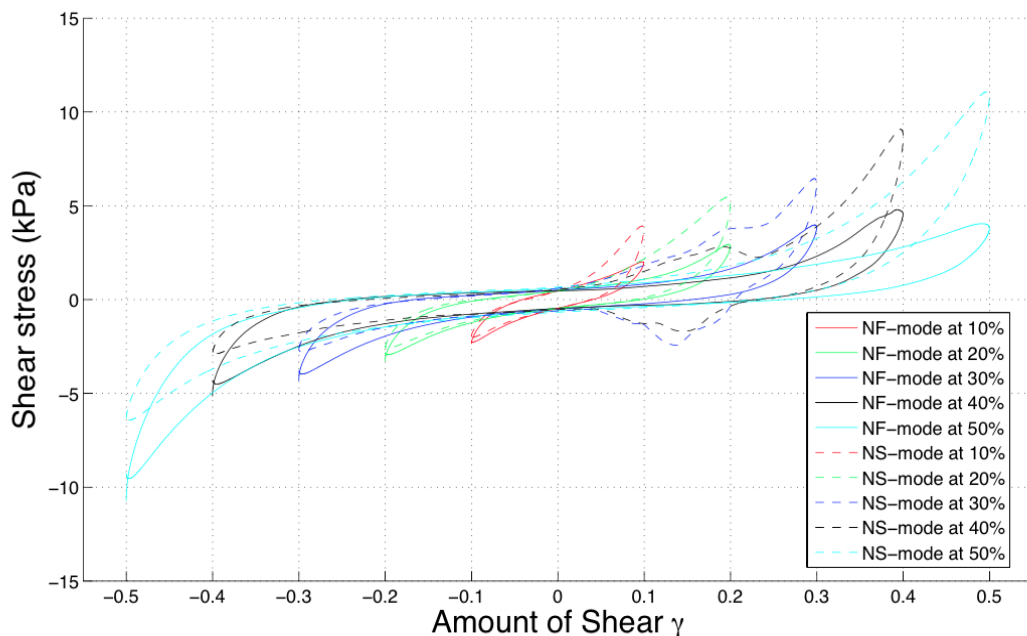


Figure 3.5: Example of a failed test (NF/NS mode of HH#32<sub>LV</sub>)

Furthermore, within SN/SF mode (see Fig. 3.6) the asymmetry can be seen. The SF-mode is higher in negative direction than in positive direction. The stress-strain curves should be symmetric to some extent. A good example therefore is the FS/FN mode (top stress-strain curve) with a nice symmetry in both modes. Whereby it is very difficult to get completely symmetric data.

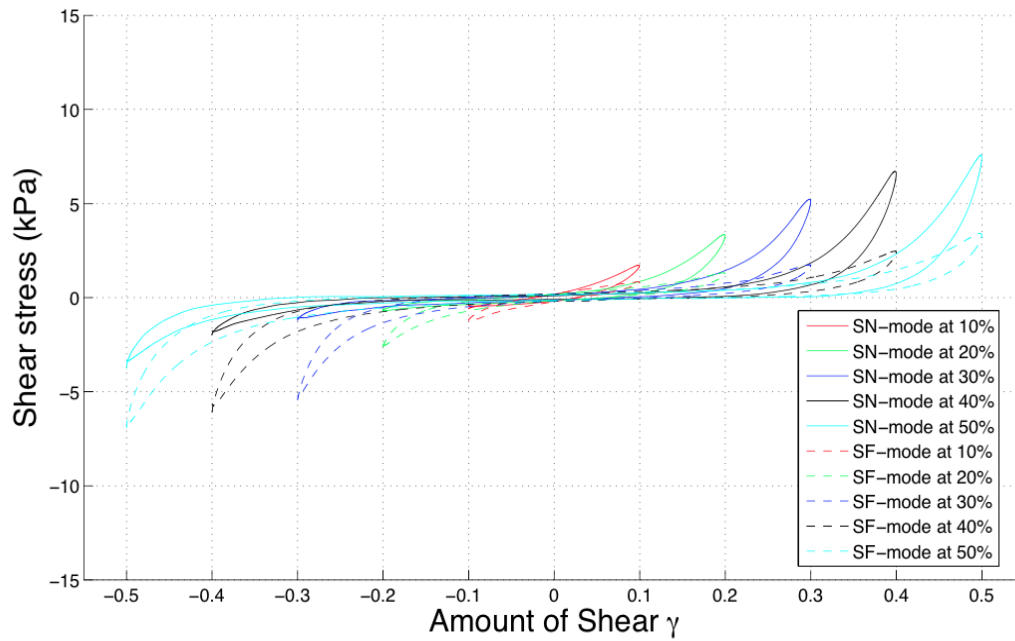


Figure 3.6: Left ventricle (HH#32) with SN/SF mode.

### 3.3 Statistical Analysis

Here the statistical analysis of the obtained data is presented for a better interpretation. Such statistical analysis is the key for the collection, analysis, interpretation, presentation and organization of data.

Table 3.2 shows a statistical overview of all eleven samples which were tested during this thesis. Included are the number of tested hearts, the sex and age of the donor and the BMI (Body Mass Index).

Table 3.2: Statistical overview of all eleven samples.

	sex %	age (yrs)	BMI (kg/m <sup>2</sup> )
Maximum	-	78	26
Minimum	-	43	24
Average	25%f, 75%m	65.9	25

This statistical analysis is presented without heart #30, #32, #36 and #37. All these hearts provided poor test data caused by different influences. Such influences could be the condition of myocardial tissue (it tends to get softer by and by) connected with the number of freezing and unfreezing and the storage time in the fridge, the preparation of the cubic specimen and the alignment with the FSN-coordinate system or the fixation of the specimen within the shear test device. Table 3.3 gives a rough overview of the reasons why these hearts were rejected.

Table 3.3: Overview of reasons of exclusion of heart #30, #32, #36 and #37.

Internal heart Index	Reason of exclusion
#30	Alignment to coordinate system failed
#32	Fixation failed - fixation dissolved at a shear strain of 30%
#36	FS/FN mode is missing - due to data loss
#37	Heating tank was broken - the test was performed at room temperature

The following figures (Figs. 3.6 – 3.14) show the average results presented in different configurations.

Figures 3.7 to 3.11 show the average results from lowest to highest shear displacement individually (0.1, 0.2, 0.3, 0.4 and 0.5 shear displacement). FN- and FS-mode show higher shear stresses at equivalent amount of shear than the four other modes. Thus, the highest resistance to shear show FS- and FN-modes, intermediate SF- and SN-modes and lowest NS- and NF-modes. There are no differences in shear stress-amount of shear relationships within the pairs of shear modes, but there is a difference in all three pairs of direction (FSFN > SFSN > NFNS).

Further, this expression seems to get stronger with increasing shear deformation. Average results and order of the shear modes become better and better with increasing shear deformation. At 10

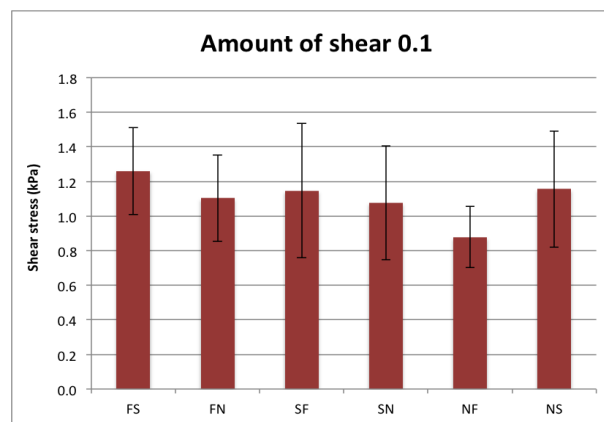


Figure 3.7: All samples for all six modes at an amount of shear of 0.1.

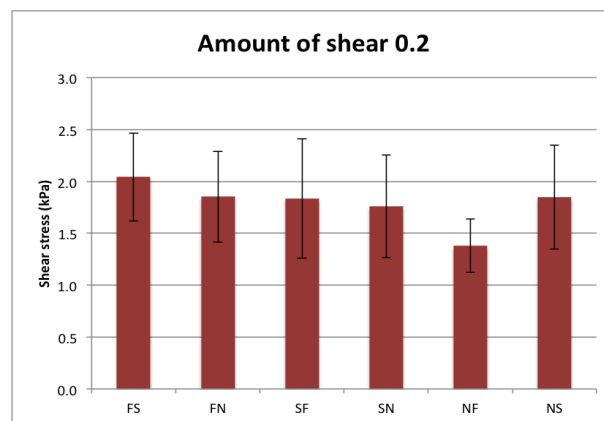


Figure 3.8: All samples for all six modes at an amount of shear of 0.2.

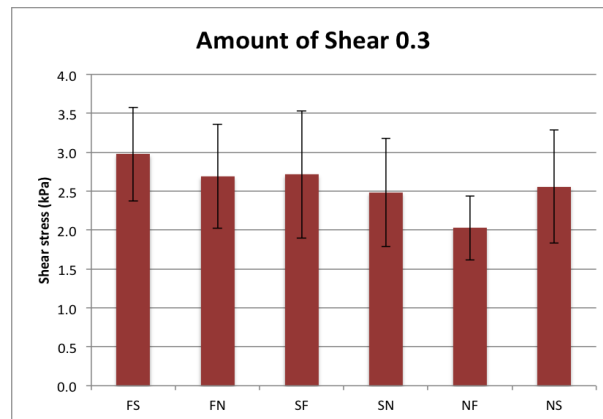


Figure 3.9: All samples for all six modes at an amount of shear of 0.3.

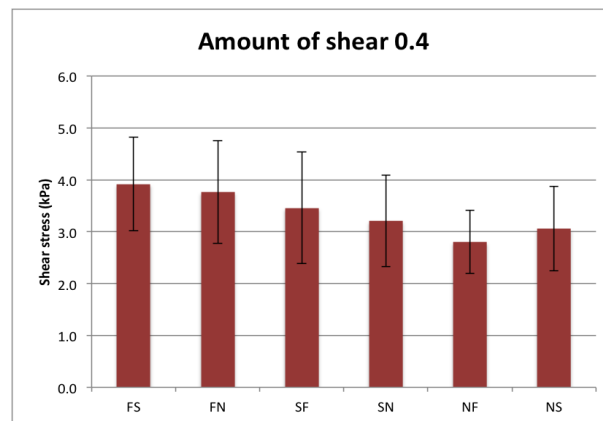


Figure 3.10: All samples for all six modes at an amount of shear of 0.4.

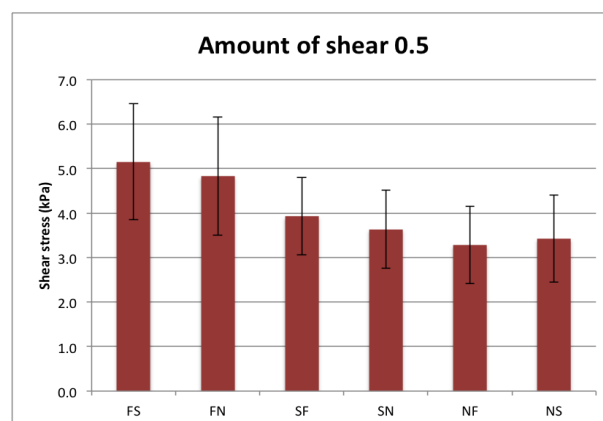


Figure 3.11: All samples for all six modes at an amount of shear of 0.5.



If you look now at the figures 3.12 to 3.14 you can see the three shear mode pairs individually. In all cases (in steps from 0.1 – 0.5 shear displacement) the FS-mode is higher than the FN-mode and the SF-mode is higher than the SN-mode the way it should be. But the NS-mode is higher than the NF-mode and not reverse in all cases, which can be seen in Fig. 3.14 and in all previous bar charts.

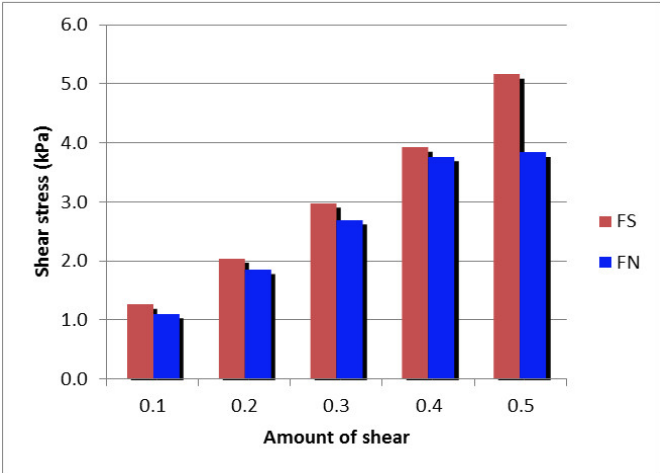


Figure 3.12: Average in FS/FN mode at 10–50% amount of shear

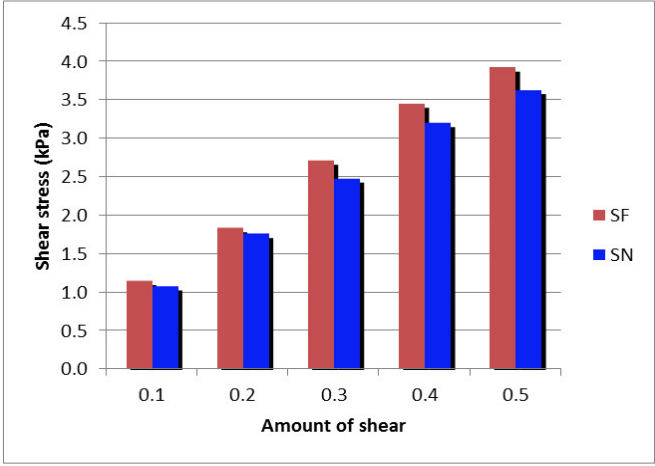


Figure 3.13: Average in SF/SN mode at 10–50% amount of shear

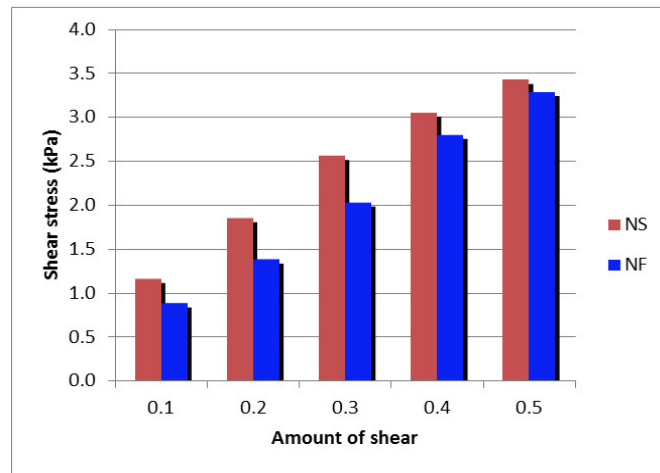


Figure 3.14: Average in NS/NF mode at 10–50% amount of shear

## 4 Discussion

The following section deals with the interpretation of the results which are presented in section 3. This includes a comparison with the results and the observed mechanical behaviour of the experiments with porcine tissue due to Dokos et al. (2002).

### 4.1 General Discussion

This work has shown that myocardial tissue has a viscoelastic, nonlinear behaviour and that it is clearly dependent on the local architecture of the myocardium. This is consistent with the work of Dokos et al. (2002).

The viscoelasticity can be explained by the hysteresis under shear deformation. Energy loss is associated with hysteresis due to frictional processes like tissue fluid movement. Thus, this hysteresis correlates with a high water content and also with the attendance of muscle. The nonlinear behaviour comes from the non-linearity of the individual components of the tissue [18]. This is commonly observed in all soft biological tissues (see section 1.2.2).

Furthermore, several more consistent properties were observed. First of all, strain softening was observed throughout the physiological range of shear deformation. To bypass this problem two preconditioning cycles were performed before the test cycle. The strain softening is explained by the minimized shear stress ( $y$ -direction) with a continuous increasing amount of shear ( $x$ -direction: from 0.1 to 0.5). Further, it can be specified by the behaviour of preconditioning and maybe by the damage of elastic components [31]. Second, myocardial tissue is anisotropic. This means that the tissue is clearly more resistant to shear deformation that is performed in a specific direction, in the direction of the myocytes (F - fiber direction). Third, the stiffness decreases in this way:  $F > S > N$  (F is the fiber orientation, S is transverse to the fiber axis within the layers, and N is the sheet normal direction) [20].

The results of this thesis demonstrate the highest stiffness in FN- and FS-modes (myocytes axis direction F perpendicular to direction of shear displacement). All four other modes are less resistant to shear. NS- and NF-modes (myocardial laminae parallel to top and bottom plates) show very low resistance to shear at all levels of shear, thus the SF- and SN-modes have intermediate properties. Summarising, the highest resistance to shear show FS- and FN-modes, intermediate SF- and SN-modes and lowest NS- and NF-modes, as you can see in Fig. 4.1. Thus, comparing this data with section 3.3 shows that the average results basically agree with already known and above characterized data and properties

of myocardial tissue. The main difference is the swap of NS- and NF-mode. In all average cases the NS-mode showed a stiffer behaviour than the NF-mode and was generally too high. Consequently, the largest mechanical stiffness shows the orientation of cardiac myofibers (F), followed by the direction of the myocardial sheets. The higher resistance to shear could be declared by the extension of the myofibers. Therefore, the sheet and fiber orientation has a contribution to the mechanical behaviour of the human ventricular myocardium [20].

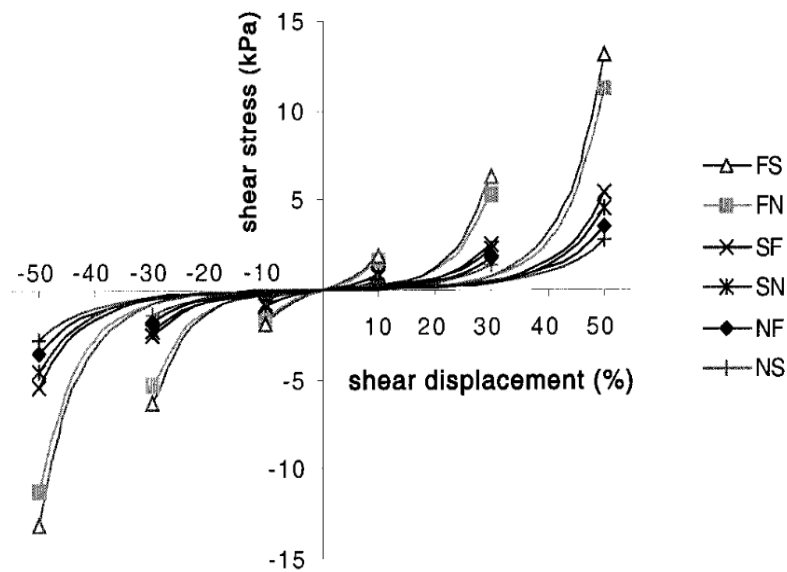


Figure 4.1: Midlines of shear stress-displacement loops averaged over all 6 hearts tested in Dokos et al. (2002). Adapted from [20].

Furthermore, you can see in Figs. 3.7 to 3.11 that average results and order of the shear modes become better and better with increasing amount of shear. At 10

The shear test device was designed for simple shear testing because simple shear is easiest to realise. In section 1.2.2 under "Simple shear" you can see the lagrangian strain tensors for all modes of shear individually. Within this context you can see the similarity of the results for the pairs of modes. For instance, the strain tensors for NF- and NS-mode. They have the same diagonal term which means extension in the direction normal to the direction of displacement, so normal to the muscle layers for this modes. The tensors only differ in the symmetrical off-diagonal shear components [20]. There are no significant differences found within the pairs of modes if we look at good data. The same can be said about the other two pairs, FN/FS and SF/SN.

As mentioned before nearly almost all samples were received frozen or were frozen because of lack of time (except of one sample of HH#29). So it can not be said that the freezing had an influence because there were no opportunities to compare fresh and frozen samples. But there was the chance to compare samples which were frozen for a short

period of time with samples which were frozen for a longer time. The amount of time that the samples were frozen had no significant influence on the results. So the freezing state has no effect on the damage of the tissue, just the freezing and unfreezing process itself. Furthermore, one thing that can be noticed is that the tissue becomes softer and is more deformable the longer it is stored in solution, for instance over night in the fridge. Tissue tend to soak up cardioplegic solution and lose their shape by and by.

## 4.2 Limitations

The structure of the myocardium was not completely uniform throughout the tested specimens and although the specimens were cut from nearly the same region, where the fiber orientation does not change steeply, the direction of the sheets on both of the surfaces (on the opposite side of the cubic specimen) was not the same. There were gradual changes in sheet orientation and a change in the fiber orientation up to  $30^\circ$  across each block. Thus, the alignment to the FSN-coordinate system was very hard and not guaranteed for all samples due to change in fiber orientation, inhomogeneities and fat inclusions in the human heart tissue. The midwall has the most uniform structure and the use of it would help to minimize this limitation [20].

Furthermore, we tested hearts in a bath with  $37^\circ\text{C}$  (to simulate a physiological environment) in a passive state. To maintain this state BDM and cardioplegic solution was used. For activation tests you would have to oxygenate the tissue during testing [20].

## 4.3 Pathological Aspects

Pathological aspects can be gender, age or heart related diseases. It was not possible to determine the effect of these factors according to the small amount of samples during this thesis. Neither it be said if age had an influence nor the BMI (Body Mass Index), because the donors had almost the same age and BMI, as you can see in Table 4.1. Further, there is no evidence that heart related diseases had an influence on the resulting data. Most of the hearts were non-failing from brain death patients, so the heart was in a good condition.

Table 4.1: Patient related heart data

Internal heart index	age (yrs)	sex	BMI (kg/m <sup>2</sup> )
#27	75	m	25
#28	43	m	24
#29	60	m	25
#30	74	m	25
#31	78	m	26
#32	73	f	-
#35	64	m	25
#36	-	-	-
#37	60	f	-
#39	-	-	-
#40	-	-	-

## 4.4 Conclusion

The results of this work are confirm with those of Dokos et al. (2002).

Summarizing, the passive human myocardium showed nonlinear, viscoelastic and anisotropic behaviour. Further, the myocardium demonstrated the highest stiffness in FN- and FS-modes, intermediate in SF- and SN-modes and the lowest in NS- and NF-modes. Thus, the order of  $FS > FN > SF > SN > NF > NS$  is fulfilled with one exception, which is the NS mode which is generally too high.

# Bibliography

- [1] Fung YC. *Biomechanics - Mechanical Properties of Living Tissues*. Second edition ed. Springer New York; 2010.
- [2] Humphrey JD. *Cardiovascular Solid Mechanics: Cells, Tissues, and Organs*. Springer; 2002.
- [3] Statistik Austria. <http://www.statistik.at/webde/presse/071153>; 2014. Todesursachenstatistik.
- [4] World Health Organization. <http://www.who.int/mediacentre/factsheets/fs317/en/>; 2014. Leading causes of death.
- [5] Hunter PJ, Smaill BH. The analysis of cardiac function: a continuum approach. 1988;52:101–164.
- [6] Sommer G, Schwarz M, Kutschera M, Kresnik R, Regitnig P, Schriefl AJ, et al. Biomechanical properties of the human ventricular myocardium. 2013;58.
- [7] Glass L, Hunter P. There is a Theory of Heart. *Physica*. 1989;43:1–16.
- [8] Arbogast KB, Thibault KL, Pinheiro BS, Winey KI, and S S Margulies. A high-frequency shear device for testing soft biological tissues. *Journal of Biomechanics*. 1997;30(7):757–759.
- [9] Schwegler J. *Der Mensch - Anatomie und Physiologie*. Thieme; 1996.
- [10] Nash MP, Hunter PJ. Computational Mechanics of the Heart. *Journal of Elasticity*. 2000;61:113–141.
- [11] Human Heart. <http://images.fineartamerica.com/images-medium-large-5/anatomy-of-heart-interior-frontal-stocktrek-images.jpg>; 2014.
- [12] Covell JW. Tissue Structure and Ventricular Wall Mechanics. *Circulation*. 2008;118:699–701.
- [13] Walker CA, Spinale FG. The structure and function of the cardiac myocyte: a review of fundamental concepts. *The Journal of Thoracic and Cardiovascular Surgery*. 1999;118:375–382.
- [14] Rohmer D, Sitek A, Gullberg GT. Reconstruction and Visualization of Fiber and Sheet Structure with Regularized Tensor Diffusion MRI in the Human Heart. 2006;.
- [15] Pope AJ, Sands GB, Smaill BH, LeGrice IJ. Three-dimensional transmural organization of perimysial collagen in the heart. *AJP - Heart and Circulatory Physiology*. 2008;295:H1243–H1252.

- 
- [16] Rohmer D, Sitek A, Gullberg GT. Reconstruction and Visualization of Fiber and Laminar Structure in the Normal Human Heart from Ex Vivo Diffusion Tensor Magnetic Resonance Imaging (DTMRI) Data. *Investigative Radiology*. 2007;42:777–789.
- [17] Holzapfel GA, Ogden RW. Constitutive modelling of passive myocardium: a structurally based framework for material characterization. *Philosophical Transactions of the Royal Society: Mathematical, Physical and Engineering Sciences*. 2009;367:3445–3475.
- [18] Holzapfel GA, Ogden RW. *Biomechanics of Soft Tissues in Cardiovascular Systems*. Springer Wien New York; 2003.
- [19] Horgan CO, Murphy JG. Simple shearing of soft biological tissues. *Proceedings of the Royal Society A: Mathematical, Physical and Engineering Sciences*. 2010;467(2127):760–777.
- [20] Dokos S, Smaill BH, Young AA, LeGrice IJ. Shear properties of passive ventricular myocardium. *AJP - Heart and Circulatory Physiology*. 2002;283:H2650–H2659.
- [21] Klabunde R. *Cardiovascular Physiology Concepts*. Wolters Kluwer; 2005.
- [22] Kramme. *Medizintechnik*. Springer; 2011.
- [23] Ziemer G, Haverich A. *Herzchirurgie: Die Eingriffe am Herzen und an den herznahen Gefaessen*. Springer; 2009.
- [24] Wikipedia. <http://de.wikipedia.org/wiki/Wikipedia:Hauptseite>; 2015.
- [25] Ostap EM. 2,3-Butanedione monoxime (BDM) as a myosin inhibitor. *Journal of Muscle Research and Cell Motility*. 2002;23:305–308.
- [26] Bond LM, Tumbarello DA, Kendrick-Jones J, Buss F. Small-molecule inhibitors of myosin proteins. *Future Science*. 2013;.
- [27] Borlak J, Zwadlo C. The Myosin ATPase Inhibitor 2,3-Butanedione monoxime Dictates Transcriptional Activation of Ion Channels and Ca<sup>2+</sup>-Handling Proteins. *Molecular Pharmacology*. 2004;66:706–717.
- [28] Backx PH, Gao WD, Azan-Backx MD, Marban E. Mechanism of force inhibition by 2,3-butanedione monoxime in rat cardiac muscle: role of [Ca<sup>2+</sup>] and cross-bridge kinetics. *Journal of Physiology*. 1994;p. 487–500.
- [29] Kutschera M. *Shear Properties of Passive Ventricular Porcine and Human Myocardium*. Institute of Biomechanics, Graz University of Technology; 2012.
- [30] Gehrman F. *A Triaxial Shear Measurement Device*. Institute of Biomechanics, Graz University of Technology; 2010.
- [31] Emery JL, Omens JH, McCulloch AD. Strain Softening in Rat Left Ventricular Myocardium. *Journal of Biomechanical Engineering*. 1997;119(1):6–12.





# Statutory Declaration

I declare that I have authored this Thesis independently, that I have not used other than the declared sources/resources, and that I have explicitly marked all material, which has been quoted by the relevant reference.

---

date

---

signature